Multiple edifice-collapse events in the Eastern Mexican Volcanic Belt: The role of sloping substrate and implications for hazard assessment

Gerardo Carrasco-Núñez [a,*], Rodolfo Díaz-Castellón [a], Lee Siebert [b],
Bernard Hubbard [c], Michael F. Sheridan [d], Sergio Raúl Rodríguez [e,f]

[a] Centro de Geociencias, Campus UNAM Juriquilla, 76230 Querétaro, México
[b] Smithsonian Institution, Global Volcanism Program, Washington, DC 20013-7012, USA
[c] U.S. Geological Survey, Eastern Mineral Resources, Reston, VA 20192, USA
[d] Department of Geology, SUNY University at Buffalo, NY 14260, USA
[e] Instituto de Geología, Ciudad Universitaria, México, D.F., 04510, México
[f] Centro de Ciencias de la Tierra, Universidad Veracruzana, Xalapa 91090, Veracruz, México

Abstract

The Citlaltépetl–Cofre de Perote volcanic chain forms an important physiographic barrier that separates the Central Altiplano (2500 masl) from the Gulf Coastal Plain (GCP) (1300 masl). The abrupt eastward drop in relief between these provinces gives rise to unstable conditions and consequent gravitational collapse of large volcanic edifices built at the edge of the Altiplano. Eastward sloping substrate, caused by the irregular configuration of the basement rocks, is the dominant factor that controls the direction of collapsing sectors in all major volcanoes in the region to be preferentially towards the GCP. These collapses produced voluminous debris avalanches and lahars that inundated the well-developed drainages and clastic aprons that characterize the Coastal Plain. Large catastrophic collapses from Citlaltépetl, Las Cumbres, and Cofre de Perote volcanoes are well documented in the geologic record. Some of the avalanches and transformed flows have exceptionally long runouts and reach the Gulf of Mexico traveling more than 120 km from their source. So far, no direct evidence has been found for magmatic activity associated with the initiation of these catastrophic flank-collapses. Apparently, instability of the volcanic edifices has been strongly favored by very intense hydrothermal alteration, abrupt topographic change, and intense fracturing. In addition to the eastward slope of the substrate, the reactivation of pre-volcanic basement structures during the Late Tertiary, and the E–W to ENE–SSW oriented regional stress regimes may have played an important role in the preferential movement direction of the avalanches and flows. In addition to magmatic-hydrothermal processes, high amounts of rainfall in the area is another factor that enhances alteration and eventually weakens the rocks. It is very likely that seismic activity may be the principal triggering mechanism that caused the flank collapse of large volcanic edifices in the Eastern Mexican Volcanic Belt. However, critical pore water pressure from extraordinary amounts of rainfall associated with hurricanes or other meteorological perturbation cannot be ruled out, particularly for smaller volume collapses. There are examples in the area of small seismogenic debris flows that have occurred in historical times, showing that these processes are not uncommon. Assessing the stability conditions of major volcanic edifices that have experienced catastrophic sector collapses is crucial for forecasting future events. This is particularly true for the Eastern Mexican Volcanic Belt, where in

* Corresponding author. Fax: +52 442 238 11 29.
  E-mail address: gerardoc@geociencias.unam.mx (G. Carrasco-Núñez).

many cases no magmatic activity was associated with the collapse. Therefore, edifice failure could occur again without any precursory warning.

1. Introduction

The quarter century since the 1980 eruption of Mount St. Helens has brought a recognition of the important role that edifice collapse plays in the evolution of volcanoes (Ui, 1983; Siebert, 1984; Francis and Self, 1987; McGuire, 1996); major edifice-failure events have now been recognized at several hundred volcanoes worldwide (Siebert, 2002). Large-scale edifice failure occurs at volcanic morphologies ranging from lava-dome complexes or small stratovolcanoes <10 km^3 in volume to massive shield volcanoes >10,000 km^3 in size (Moore et al., 1989; Siebert, 2002). Typically less than 10% of an edifice fails, but repeated failures can occur as renewed eruptions reconstruct the edifice. The ensuing volcanic debris avalanches travel far beyond the flanks of a volcano (<10 to >100 km) at velocities that may approach 100 m/s, covering areas of <10 to >1000 km^2. Edifice collapse can occur in association with magmatic and/or phreatic eruptions, or in the absence of eruptive activity, complicating the identification of precursory phenomena. Morphology, textures and emplacement mechanisms vary with water content; avalanches can be relatively dry, or in some instances sufficiently wet to transform into lahars that can travel longer distances and cover broader areas.

In Mexico edifice collapse phenomena have been identified at several major volcanoes within the Mexican Volcanic Belt (MVB), as summarized by Capra et al. (2002). In particular, edifice collapses of the Citlaltépetl–Cofre de Perote Volcanic Range (CCPVR), situated in the Eastern MVB, have preferentially been directed eastward towards the Gulf of Mexico coast. We will present evidence that this particular direction of collapse is mainly controlled by the sloping substrate, and is favored by other factors causing instability such as abrupt relief, tectonic setting, and hydrothermal alteration.

The purpose of this study is to describe the occurrences of edifice collapse deposits originating from the CCPVR, to explain the preferential distribution of past debris avalanches and debris flows deposits along the eastern side of the range, and to discuss different factors that could be assumed to favor unstable

conditions and control the edifice failures. In particular, we emphasize that future hazard assessments should consider those cases where edifice collapse may occur without any associated volcanic activity, and thus they may not provide a warning or any precursory activity.

2. Regional geologic and physiographic setting

The Mexican Volcanic Belt (MVB) is an irregular province, about 1000 km long and 20–150 km broad, that lies oblique to the Middle American Trench, and extends east–west between Veracruz (Gulf of Mexico) and Puerto Vallarta (Pacific Ocean) (Mooser, 1972; Demant, 1978; Ferrari et al., 1999). The MVB consists of a wide variety of volcanic structures, including large stratovolcanoes, various silicic complexes and calderas, large monogenetic fields, isolated silicic domes, and abundant scattered volcanoes. The magmas are mainly calc-alkaline, ranging from basalt to rhyolite in composition. A characteristic feature of the MVB is the occurrence of high-relief, nearly north-south trending volcanic ranges formed by large stratovolcanoes, separated by wide intramontane lacustrine/playa basins containing flank collapse deposits, as well as other minor volcanoes (Capra et al., 2002).

The eastern MVB comprises the Serdán-Oriental basin and the CCPVR (Fig. 1). The Serdán-Oriental basin is a broad, internally drained, intermontane basin of the Mexican High Plain (Altiplano). It is characterized by monogenetic bimodal volcanism that has produced isolated relatively large rhyolitic domes and small, isolated cinder, scoria, and lava cones of basaltic composition, and some maar volcanoes including mostly tuff rings, a few maars sensu stricto, and a few tuff cones.

Cretaceous limestones and shales form the regional basement of the Eastern MVB (Yáñez and García, 1982). These rocks make up a conspicuous NW–SE-trending folded and faulted mountain range that is partially covered by Quaternary calc-alkaline volcanics of the E–W-trending Mexican Volcanic Belt.

The CCPVR forms an important physiographic divide separating the Altiplano (Serdán-Oriental basin) to the west from the GCP to the east. These contrasting
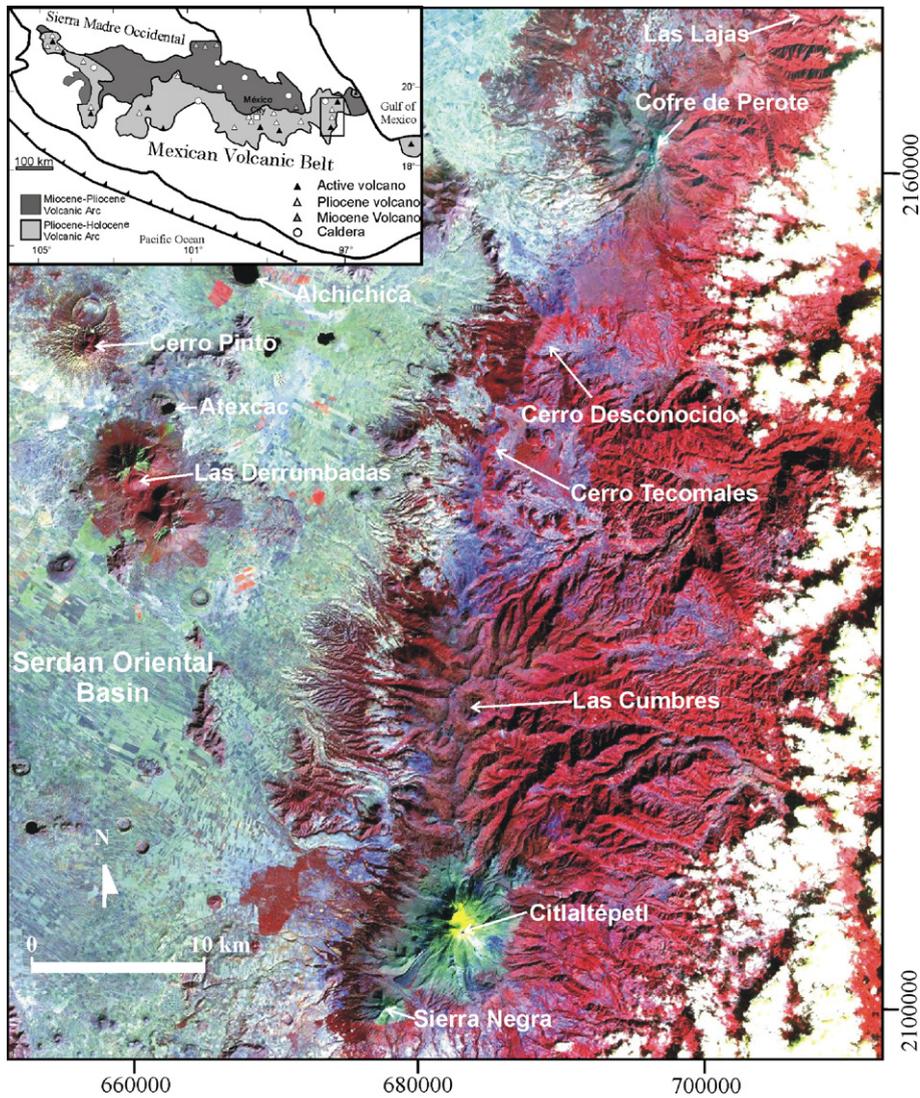
Fig. 1. Thematic Mapper satellite image of the eastern Mexican Volcanic Belt (MVB) courtesy of M. Abrams at Jet Propulsion Laboratory, USA. Inset box shows image location in the MVB.

geomorphic provinces have important implications for drainage development on either side of the CCPVR because of their distinct climatic conditions. For example, the GCP has a well-developed and integrated drainage network with deep stream incision and gullies, V-shaped valleys and permanent streams. This is due to the very high rates of precipitation on the eastern flanks that produce a wet sub-tropical climate that enhances secondary alteration and favors soil development towards the coastal plains. In contrast, the Serdán-Oriental basin is characterized by an arid climate with low rainfall rates that does not support an integrated drainage network, and its landscape is dominated by ephemeral streams, shallow lakes, and salt pans.

3. Citlaltépetl–Cofre de Perote Volcanic Range (CCPVR)

The CCPVR consists of a wide variety of volcanic centers forming the 70-km long, nearly N–S trending chain that includes several large stratovolcanoes, minor cinder cones, and a few silicic domes. The varied morphologic characteristics of the volcanic structures show different degrees of erosion and indicate a relative southward younger age of the volcanism. There are two main alignment directions: a NE–SW trend containing the northernmost Las Lajas–Cofre de Perote–Cerro Desconocido volcanoes, and a N–S trend with the Cerro Deconocido–Las Cumbres–Citlaltépetl volcanoes (Fig. 1).

Cofre de Perote is a 4200-m-high, andesitic stratovolcano that exhibits a prominent scarp at the summit. Its activity started at about 1.6 Ma (Cantagrel and Robin, 1979) and continued during the Late Pleistocene times. Dacitic lava flows of the summit area have a K/Ar date of 0.24 ± 0.05 Ma and apparently mark the end of its activity (Lozano and Carrasco-Núñez, 2000).

Cerro Desconocido and Cerro Tecomales, which are of probable Plio-Pleistocene age, form the La Gloria Volcanic Complex. Due to their morphology (see Fig. 1), they have been regarded as eroded calderas (Negendank et al., 1985); however, we have found no evidence to support that hypothesis, so for the present they can be considered as an eroded chain of aligned vents.

Las Cumbres volcano shows a circular summit depression about 4 km in diameter with a central dome. The morphology of the summit area suggests an origin related to an explosive caldera (Höskuldsson, 1992), but more recent work (Rodríguez-Elizarrarás, 2005) interprets this feature to be a horseshoe-shaped amphitheater formed by a catastrophic collapse and later filled in with a dacite lava dome that extends to a height above the breached rim. This volcano has been eroded by glaciers (Heine, 1988) and is proposed to be of Late Pleistocene age (Rodríguez, 1998).

Citlaltépetl, also known as Pico de Orizaba, is North America's highest volcano (5685 m) and Mexican's highest peak. This ice-capped, andesitic stratovolcano, located at the southern end of the CCPVR, is the only historically active volcano in the area. Its most recent
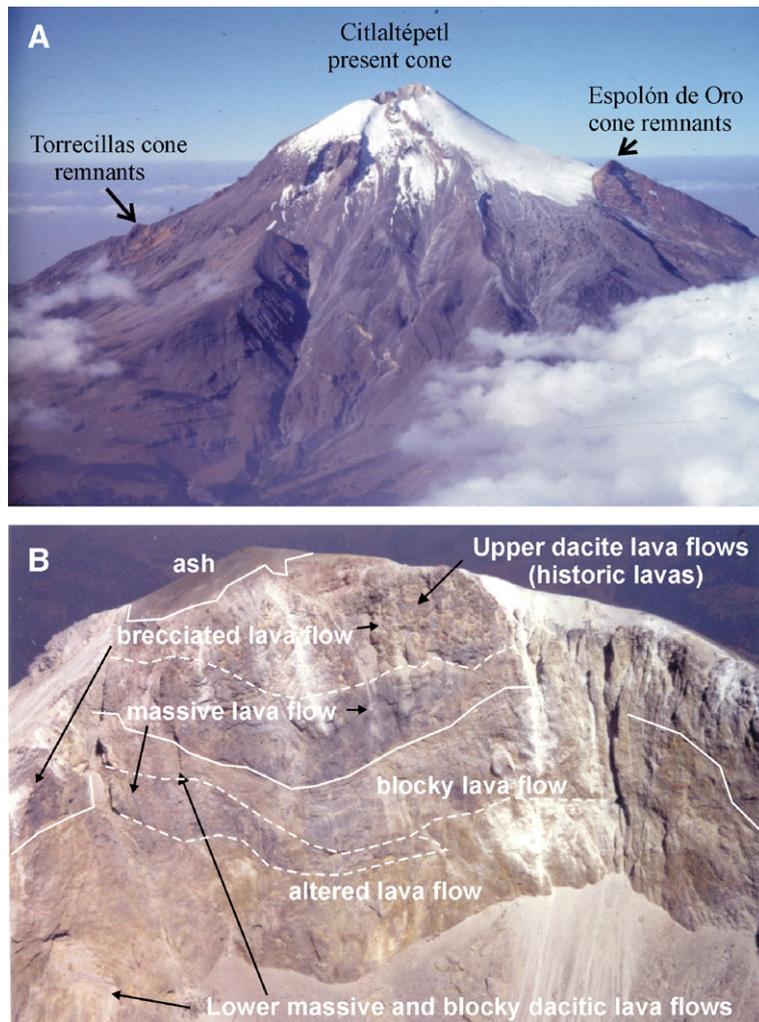

Fig. 2. Photographs of Citlaltépetl volcano. (A) Panoramic air photo of Citlaltépetl showing the present cone and the ancient cone remnants. (B) View of the interior of Citlaltépetl's crater showing areas of fresh and altered rocks.

activity was reported in 1867 (De la Cruz-Reyna and Carrasco-Núñez, 2002). Carrasco-Núñez (2000) proposed that the modern edifice of Citlaltépetl volcano consists of three superimposed stratovolcanoes and dome intrusions (Fig. 2A). The cone-building stages include: the Torrecillas (650–250 ka), Espolón de Oro (210–16 ka), and Citlaltépetl (16 ka to present) stages (Fig. 3). Of note, remnants of the Espolón de Oro stage show evidence of deep glacial erosion with prominent cirques on its western flanks (Heine, 1988).

About 7 km southwest of Citlaltépetl is Sierra Negra Volcano, a 4650-m-high andesitic stratovolcano which first erupted during the Pleistocene and has a possible age of about 0.5 Ma (Höskuldsson, 1992). Sierra Negra is not aligned in the main N–S volcanic trend, but has a local lineament with Citlaltépetl and some dacitic domes along a NE–SW direction. Some additional dacitic and rhyolitic domes are situated between the Las Cumbres and Citlaltépetl centers with no particular alignment.

3.1. Multiple collapsing events at the CCPVR

Because the CCPVR forms an important topographic barrier separating the ∼2500 m asl Serdán-Oriental basin from the <1300 m asl GCP, the abrupt drop in relief between the two physiographic provinces favors unstable conditions and gravitational collapse of the large volcanic edifices like Citlaltépetl, Las Cumbres, and Cofre de Perote. There have also been several small-scale landslides and debris flows in Holocene times, some of which are not related to the activity of the large volcanoes (e.g. the 1920 seismogenic event). There are also a few isolated exposures of other volcaniclastic deposits, but their sources remain unknown.

The geologic record of these volcanoes show that several catastrophic edifice collapses have occurred, and in the cases of Citlaltépetl and Cofre de Perote there have been multiple events. Some of the resulting avalanches and transformed flows have exceptionally long runouts and reach the Gulf of
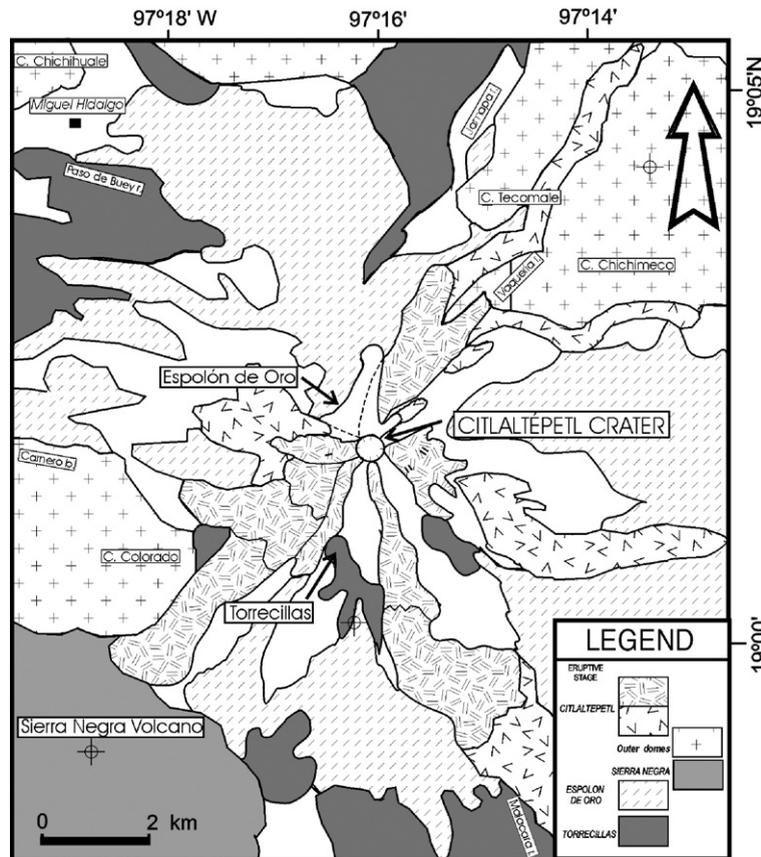

Fig. 3. Simplified geologic map of Citlaltépetl volcano showing the three main eruptive stages and the surrounding volcanic features (outer silicic domes and Sierra Negra volcano) modified from Carrasco-Núñez (2000).
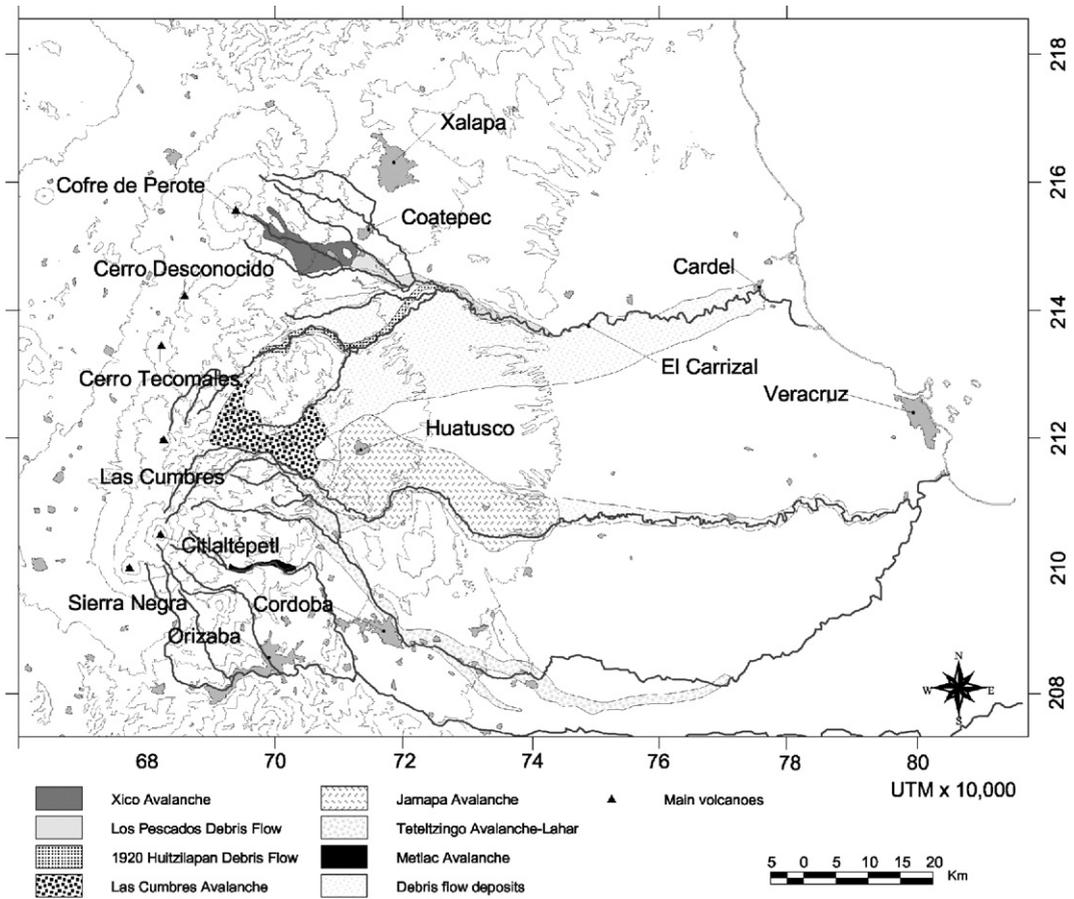
Fig. 4. Distribution of the main debris-avalanche and debris-flow deposits derived from the Citlaltépetl–Cofre de Perote Volcanic Range.

Mexico after traveling more than 120 km from their source, mainly as hyperconcentrated flows. All the major debris avalanche and debris flow deposits resulting from edifice failures along the CCPVR are located in the coastal plain (Fig. 4) and are described below.

4. Citlaltépetl volcano

Since late Quaternary time, the volcano has shed considerable amounts of volcaniclastic debris on its flanks and into the river valleys that drain it, including voluminous avalanches, lahars and other debris flows. Originally Höskuldsson et al. (1990) claimed the existence of four debris avalanches associated with the Citlaltépetl volcano. However, further investigations (Carrasco-Núñez, 1993; Siebe et al., 1993; Carrasco-Núñez et al., 1993) verified the existence of only two major voluminous deposits (Jamapa avalanche and Teteltzingo lahar) that are related to collapses of ancestral volcanoes above which the present cone

grew (Fig. 2). In addition to those large deposits, a comparatively small-scale debris avalanche deposit located about 20 km southeast of the volcano crops out along the Metlac river-valley.

4.1. Jamapa avalanche

About 250 ka the ancient Torrecillas cone collapsed, forming a ca. 3.5-km-wide breached crater. This produced the Jamapa avalanche, a voluminous (ca. 25 km^3) debris avalanche and debris flow that covered an area of about 350 km^2. It traveled 75 km as a primary avalanche (Carrasco-Núñez and Gómez-Tuena, 1997) after which it transformed to a lahar that terminated at the Gulf coast as a secondary hyperconcentrated flow. At least two different horizons comprise the whole debris avalanche deposit, which is heterolithologic, massive and shows highly altered zones in many areas with gravels and boulders supported within a silty–clayey matrix. At about 35 km northeast from Citlaltépetl volcano, in the Huatusco area, the surface

of the deposit exhibits an irregular hummocky topo-graphy (Fig. 5).

The alteration mineralogy of the pre-collapse Torrecillas edifice is comparable to that of the Jamapa avalanche deposit in that they both contain abundant kaolinite, ferric-oxyhydroxide minerals, and high-temperature silica minerals, such as hydrous forms of quartz, cristobalite and tridymite, not normally found in abundance in andesitic rocks (Hubbard, 2001). In addition, smectite and the sulfate minerals alunite and jarosite occur in samples of altered rocks collected from Torrecillas (Hubbard, 2001). A similar mineral assemblage, with the addition of pyrite and native sulfur, was reported at Soufrière Hills volcano (Boudon et al., 1998). The uppermost outcrops of Torrecillas stage rocks are heavily fractured, silicified and erosion-resistant despite their being the most intensely altered parts of the volcano. Hubbard (2001) proposed that an advanced argillic alteration zone existed above the level of exposed Torrecillas stage rocks, which ultimately became incorporated into the Jamapa avalanche deposit.

4.2. Metlac avalanche

This is a small debris avalanche deposit, probably less than 1 km³, which fills the Metlac valley with a thickness of more than 100 m, but has a very limited distribution (Fig. 4). It is an indurated, massive, bouldery-rich, matrix-supported, heterolithologic deposit, which is dominated by andesitic clasts. The deposit has a very irregular and conspicuous shape due to erosion along its margins on both sides of the main river-valley. This morphology may suggest that the deposit is relatively old, however, there are no dates for this deposit. It contains many jigsaw-fractured blocks, about 0.5–1 m in diameter. This avalanche seems to have transformed to a debris flow downstream, probably caused by the failure of a temporary dam that was formed when the Metlac debris avalanche partially blocked the drainage.

4.3. Teteltzingo avalanche-lahar

During the Late Pleistocene, the ancestral Espolón de Oro cone collapsed, and the resulting avalanche rapidly transformed into a lahar that filled the confined drainage and deposited extensive flat terraces that show only a few scattered small (up to 15 m high) hummocks. Rocks from the Espolón de Oro source area are highly fractured and altered to argillic and advanced argillic assemblages in their uppermost exposures, grading downward to less fractured and fresher units within 400 m of the more altered horizons (Fig. 6A).

The Teteltzingo avalanche-lahar appears to be a single massive, unbedded, poorly sorted mixture of heterolithologic pebbles, cobbles, and boulders sup-ported within a characteristic yellow-brown, clayey, silty sand matrix (Fig. 6B) that contains small vesicles suggestive of air bubbles trapped in a water-saturated matrix. The deposit is 12–20 m thick on average, but in a few places is up to 100 m thick. Veneer deposits extend up to 60 m above the terrace level in proximal facies. This clay-rich lahar contains 10–16% of secondary alteration minerals such as smectite, and kaolinite, an assemblage that is comparable with other cohesive lahars such as the Osceola lahar (formerly "mudflow", Crandell, 1971) that originated from the collapse of

Fig. 5. Photograph showing a 5-m high hummock of the Jamapa avalanche in the Huatusco area (see Fig. 4 for location).
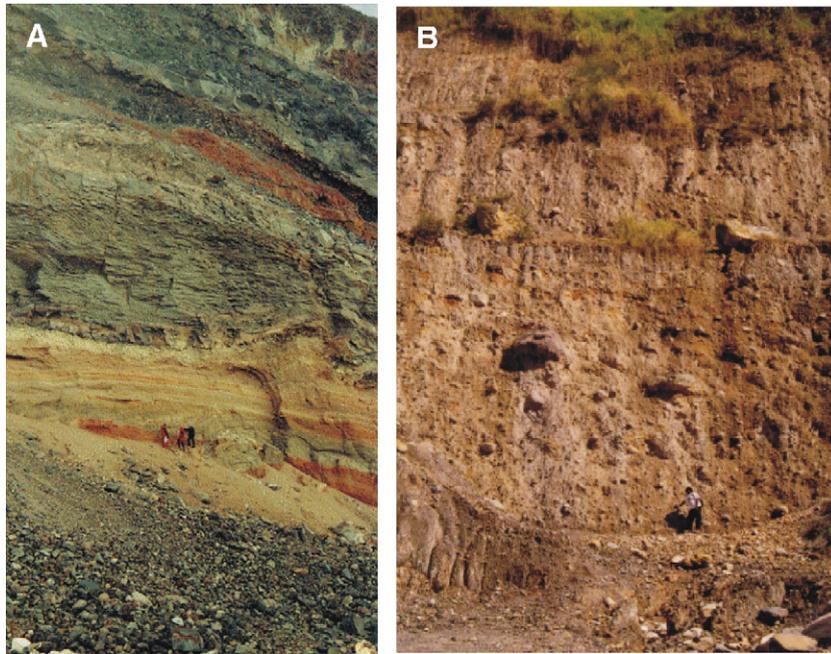
Fig. 6. Photographs of the Teteltzingo avalanche-lahar deposit and its source area. (A) The upper remnants of the Espolon de Oro peak, the source area for the Teteltzingo lahar showing highly altered layers that alternate with fresh lava flows. (B) A 25-m-thick massive clay-rich deposit near Cordoba City, at a distance of about 45 km from source, but still containing very large blocks.

unstable edifice of ancestral Mount Rainier (Crandell, 1971). Hubbard (2001) studied the alteration mineralogy of the Espolón de Oro and the Teteltzingo deposits and found comparable assemblages containing: opal, cristobalite, hematite, goethite, alunite, jarosite, gypsum, anhydrite, kaolinite and smectite.

The Teteltzingo lahar extends at least 110 km from its source to the coast, covers an area of 175 km^2 east of the volcano, and has a volume of 2.2 km^3. These values are higher than those estimated previously (Carrasco-Núñez et al., 1993) who report a distance of 85 km, an area of 143 km^2, and a volume of 1.8 km^3. Carrasco-Núñez et al. (1993) inferred an age ranging between 13 and 27 ka, however, direct radiocarbon dating on large fragments of wood samples within the deposit near the city of Cordoba provided an age of 16,550+145/−140 for the lower part, and 16,365±110 for the upper part of the deposit.

The deposit's features suggest that it had an origin as a sector collapse of hydrothermally altered rock that transformed from a debris avalanche to a cohesive lahar very close to its source, similar to the Osceola lahar (Vallance and Scott, 1997). Carrasco-Núñez et al. (1993) proposed that the presence of glacier ice and a very active hydrothermal system during late Pleistocene time provided a constant supply of pore water, which enhanced the hydrothermal alteration of the summit of
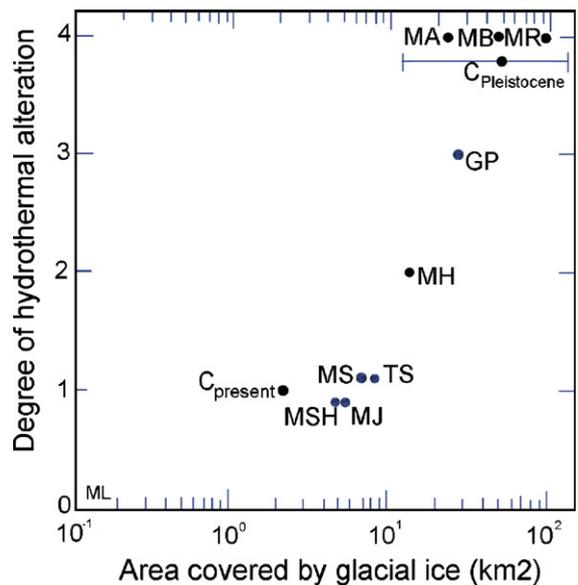

Fig. 7. Plot of the degree of hydrothermal alteration versus the area covered by glacial ice for the Cascade volcanoes and Citlaltépetl (from Carrasco-Núñez et al., 1993). 0—no alteration; 1—small areas of moderate alteration; 2—moderate alteration; 3—large areas of moderate alteration; 4—large intensely altered rocks. C—Citlaltépetl, GP—Glacier Peak; MA—Mount Adams; MB—Mount Baker; MH—Mount Hood; MJ—Mount Jefferson; ML—Mount Lassen; MR—Mount Rainier; MS—Mount Shasta; MSH—Mount St. Helens; TS—Three Sisters.

Citlaltépetl and was the origin of most of the water for the lahar. The intense hydrothermal alteration seems to be related to an acid-sulfate leaching process where sulfates are added, while mobile elements are removed from the surroundings rocks to form clay, silica, and sulfate minerals (Frank, 1983). An empirical estimation of the degree of hydrothermal alteration based on the area and intensity of that alteration was used by Carrasco-Núñez et al. (1993) to correlate with the area covered by glacial ice (Fig. 7). These observations suggest that glaciated volcanoes are sites where hydrothermal alteration and resulting cohesive lahars are most likely. The effects of the glaciation on active stratovolcanoes are twofold: (1) they enhance the exposure of hydrothermally altered rocks, often by eroding away fresher and stronger rocks, and (2) they enhance the process of alteration by supplying a slow, steady supply of water above the water table, which allows for small to moderate fluxes of concentrated acidic fluids (Carrasco-Núñez et al., 1993).

5. Las Cumbres

Las Cumbres, located approximately 10 km north of Citlaltépetl volcano, is an eroded stratovolcano consisting of thick and massive lava flows of andesite composition (Rodríguez-Elizarrarás, 2005). The present summit rim (3800 m asl) marks the boundary of a 4 km diameter collapse caldera that is breached to the east. The maximum height of the pre-collapse stratovolcano could have been similar to that of the present Citlaltépetl volcano (5675 m asl) because these two volcanoes have a similar base diameter of about 20 km (Rodríguez, 1998). All lavas in the Las Cumbres stratovolcano contain abundant hornblende and may be classified principally as hornblende pyroxene andesites.

The partial collapse of the eastern flank of Las Cumbres volcano occurred between 40,000 and 350,000 years ago, based on stratigraphy. Some radiometric dates for the younger deposits were made by the C-14 method (Rodríguez-Elizarrarás, 2005) and those for the older lavas by the Ar/Ar technique (Sheridan, unpublished data). The horseshoe-shaped structure formed by the flank collapse later was partially filled by a lateral lava flow that rests upon the debris avalanche deposits. Volcanic activity at this volcano ended with the emplacement of a dacitic dome within the caldera. This stratigraphy apparently suggests that the collapse could have been related to magmatic activity. The present morphology of the summit area with truncated hanging U-shaped valleys is the result of erosion during the last glaciation epoch (Heine, 1988).

5.1. Cumbres debris deposits

The flank collapse of Las Cumbres produced a huge debris avalanche deposit (Rodríguez, 1998; Hubbard, 2001; Scuderi et al., 2001; Rodríguez-Elizarrarás, 2005) that has an eastward distribution along the Huitzilapan-Pescados drainage basin (Fig. 4). Hubbard (2001) estimated a volume for the missing part of the Las Cumbres volcano as $>8.1 \times 10^{10}$ m^3 (≈ 80 km^3). Field mapping by Childs (2005) expanded the boundaries of the deposit to yield an area of 1500 km^2 and estimated a volume of 60 km^3 by constructing about thirty 3D polygons with thicknesses that were constrained by measured sections and flow margins. This heterolithologic and massive debris deposit largely transformed from an avalanche to a debris flow at approximately 20 km from the caldera. Much further along its path, near the Gulf of Mexico coastline 120 km distant, it possibly changed into a hyperconcentrated flow.

The Las Cumbres debris deposit appears to form a single continuous stratigraphic horizon linking the debris avalanche beds with the debris flow deposit. No inter layering or erosion hiatus is present between deposits with these two different textures. Because terraces capped by both types of deposits follow a single continuous gradual gradient back towards the volcano, the outer limits and thickness of the deposits can be mapped with some degree of confidence. Both the avalanche and the debris flow deposits show different features, so they are described separately.

5.1.1. Cumbres avalanche deposit

In proximal zones (Fig. 4), the avalanche deposits are thicker than 100 m and contain boulder-sized clasts with highly altered areas (Fig. 8) and jigsaw-fractures. In proximal exposures an interbedded sequence of lavas and andesitic pyroclastic flows rest upon the avalanche deposit.

Imbricated and brecciated blocks of the source volcano within the avalanche deposit range in size from a few centimeters to 6 m in long dimension. The highly angular clasts are generally monolithologic hornblende andesites. Jigsaw fractures are prevalent within all clast sizes. Microcracks in the Las Cumbres debris avalanche clasts, similar to those described by Komorowski et al. (1991) for the Mount St. Helens debris avalanche, occur in both crystals and in glass. Hackly morphology in the Las Cumbres clasts consisting of abundant overlapping attached scales probably resulted from pounding of grains during repeated episodes of rapid compression and dilation during transport. In some locations, such as near the junction

Fig. 8. Photograph of Las Cumbres Avalanche deposit in a proximal area, about 12 km from source, showing the chaotic distribution of clasts and highly altered areas. The white bar is 2 m long.

between the Huitzilapan and Los Pescados Rivers, the deposit contains yellowish strongly altered areas. X-ray analysis revealed the presence of illite/smectite (Childs, 2005) in some samples and kaolinite in others (Hubbard, 2001; Childs, 2005). In this location the avalanche deposit is at least 300 m thick, the base not being exposed at river level.

5.1.2. Cumbres debris flow deposits

The Las Cumbres debris flow deposit is a massive, ungraded, volcaniclastic unit containing abundant large clasts of hornblende andesites (Childs, 2005). At several locations the deposit consists of two massive beds separated by a thin parting. No prominent erosion, discontinuity, or soil exists between these beds suggesting that the two beds probably represent individual lobes or pulses related to the same catastrophic collapse event. In medial areas south of the Pescados River this deposit rests upon a Pleistocene ignimbrite; north of the river it lies above older basaltic lavas or Cretaceous limestones. Generally this horizon is capped only by a thin soil or fluvial gravels. At higher elevations westward towards the source it is deeply dissected by the Pescados and Huitzilapan rivers where it forms relatively flat terraces and mesas up to 300 m above the channels. The mesa-capping debris flow facies crops out continuously for several tens of kilometers in the medial and distal areas.

Approaching the coast the debris flow terraces become systematically lower along the Pescados River. In this zone it forms a massive horizon with an indurated sandy matrix that is generally between 20 and 10 m thick. Gravel and small boulders are dominantly hornblende bearing andesites, but extraneous lithologies that are absent in the avalanche deposits, such as limestone and basalt, are common due to their incorporation into the debris flow by downstream bulking.

In contrast with the avalanche deposit, boulders in the debris flow do not contain jigsaw fractures and the matrix material is more strongly indurated. An exception to this rule is an exposure on the bank of the Pescados River beneath the south end of the foot bridge leading from the thermal pools at El Carrizal. Here the rock textures are typical of avalanche deposits with angular jigsaw-fractured blocks set in a strongly cemented matrix. Although this exposure is at the same stratigraphic horizon and contains the typical hornblende hypersthene andesite lithology of the Las Cumbres deposits, the mechanism for its transport to this location is an enigma. Perhaps this exposure represents a large coherent hummock of debris avalanche that was incorporated into the more mobile debris flow and dragged to this location. The Naranjo Debris Flow derived from the collapse of Nevado de Colima volcano contains hummocks incorporated by the lahar as far as 100 km from the source (Capra and Macías, 2002). Alternatively it could represent another avalanche that is yet undescribed. However, the great distance form the source (∼80 km) weakens the latter hypothesis. Clasts within all other exposures of the

debris flow beds are highly rounded and vary in size from sand and clay to a meter across.

At distal areas, the deposit has a thickness between 20 and 10 m and contain gravels (1–5 cm) and small boulders of hornblende bearing andesitic lavas. In places it is cemented and has limestone clasts; in other cases, the deposit forms terraces and contains small angular lava boulders embedded in a sandy matrix.

6. La Gloria–Huitzilapan

The Huitzilapan River, which drains into the Pescados, is one of several watersheds draining the eastern flanks of the CCPVR. The upstream source area of this drainage consists of two eroded volcanic centers that comprise La Gloria Volcanic Complex, Cerro Tecomales in the southern part and Cerro Desconocido in the northern part. The morphology of this area is comprised of steep sided mountains, which form the walls of the Huitzilapan and Pescados River. These uplands consist of faulted and folded massive limestones in the middle and lower reaches. In the upper parts of the valleys, thick andesitic lava flows and pyroclastic fall and flow deposits are the predominant materials. Fracture systems in the region have three main orientations: E–W, NW–SE and ENE–SSW, the last one coincides with the propagation direction of the 1920 earthquake and is therefore considered young and active.

Deposits of two large Holocene debris flows are exposed within the lowest terrace (Fig. 9). The youngest of these two deposits was triggered by an estimated 6.5 magnitude earthquake in 1920 (Singh et al., 1984), which was preceded by 10 days of heavy rainfall (Oddone, 1921; Camacho and Flores, 1922). Based on the 40–65 m high water mark of the flow and the lahar inundation model of Iverson et al. (1998), Hubbard (2001) estimated a volume of 0.044 km^3 for the flow. According to eyewitness descriptions (Camacho and Flores, 1922), the debris flow inundated several villages during the first 20 km (leaving 10 m thick deposits) after which it transformed into a hyperconcentrated flow downstream.

This debris flow was similar in magnitude and origin to the 1994 earthquake-triggered Paez debris flow, Colombia (Martínez et al., 1995; Scott et al., 2001) and the 1998 Casita lahar, Nicaragua (Scott et al., 2005). The 1920 Huitzilapan debris flow began as small, shallow landslides that dammed tributaries to the Huitzilapan River (Fig. 10) coalesced to a single flow, and bulked with stream materials to generate an even larger floodwave. The main debris flow phase traveled nearly 30 km downstream. Despite the regrowth of vegetation since 1920, numerous failure scarps are still visible in the limestone uplands.

The 1920 Huitzilapan deposit (Fig. 9) consists of dispersed pebble- and cobble-sized clasts supported in a sandy-silty matrix, with no grading or stratification. Some of the well-rounded clasts were clearly bulked into the debris flow from the stream sediments. Many of the clasts are sub-rounded to sub-angular, indicating that they did not travel far from their source. The diameter of the largest measured boulder in the deposit was 110 cm (Fig. 9).

Fig. 9. Photograph showing the 1920 Huitzilapan deposit overlaying the 5860± yr B.P. debris flow deposit along the Huitzilapan river-valley. Dashed line indicates the contact between these two deposits.
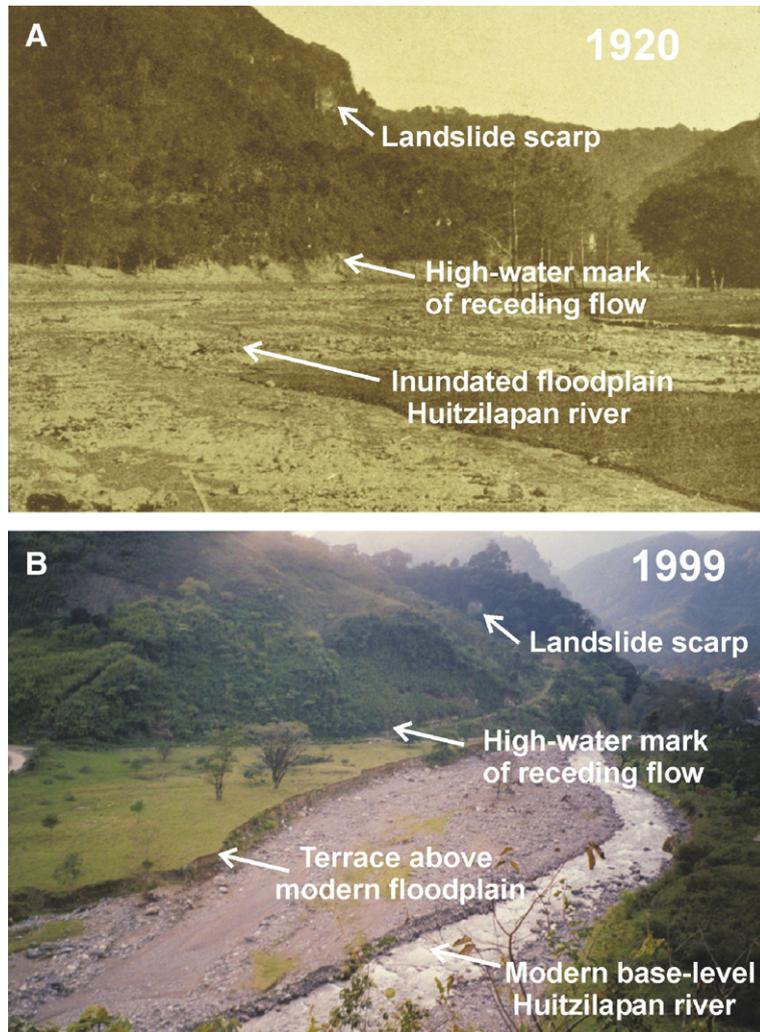
Fig. 10. Comparison of photographs of the 1920 seismogenic debris flow taken in 1920 and 1999, showing some landslide scarps and the lower terrace formed by the 1920 seismogenic debris flow along the Huitzilapan River.

Wood collected within the older debris flow deposit yielded a radiocarbon age of 5260+45 yr B.P. Grain-size analysis of the matrix from both deposits indicates that they contain >5% clay-sized materials, which suggests that they were both emplaced by cohesive debris flows. The clay-sized fractions of both deposits were further studied using X-ray diffraction, infrared spectroscopy, and scanning electron microscopy. The matrix of the 1920 Huitzilapan seismogenic debris flow deposit contains spherical halloysite and opaline silica, which were most likely derived from soils and intensely weathered volcanic deposits that occur throughout the watershed. The matrix of the older debris flow deposit contains platy, well-crystalline kaolinite, which suggests a hydrothermal alteration origin rather than chemical weathering. The nearest source of kaolinite is repre-

sented upstream by hydrothermally altered ash deposits exposed on the eastern flanks of a post-caldera rhyolite dome dated at 5860+60 yr B.P. (Rodríguez, 1998). Additional fieldwork is needed to constrain the extent of this debris deposit, which appears to be comparable in size and magnitude to the 1920 deposit.

7. Cofre de Perote

The summit area of the andesitic Cofre de Perote composite volcano is characterized by a prominent set of scarps that as a group show a spectacular horseshoe shape (Fig. 11A) that may be linked to repetitive flank failures. So far, at least two main debris avalanche deposits have been confirmed on the eastern lower slopes of Cofre de Perote towards the GCP (Fig. 4).

Fig. 11. Photographs of the Xico avalanche and its source area. (A) View of the eastern flank of Cofre de Perote summit area showing the horseshoe-shaped amphitheater. (B) Outcrop at about 10 km from source showing the massive and chaotic nature of the Xico avalanche deposit with large blocks within a silty matrix.

These deposits are exposed along the Los Pescados River drainage that empties into Veracruz harbor.

7.1. Xico avalanche

Preliminary studies of the Xico avalanche deposit reveal a massive, heterolithologic, boulder-to-gravel-sized deposit with a silty–clayey matrix (Fig. 11B). The deposit extends at least 20 km from source and is mainly confined along the river valley. However, locally it spreads laterally to partially cover the surrounding topography, leaving only some paleotopographic high

areas uncovered. Some large megablocks in proximal areas somewhat resemble enormous toreva blocks (Reiche, 1937) that still preserve the original structure of the edifice.

Radiocarbon dating of pieces of charcoal from within the deposit provide an age of about 10,000 yr B.P., much younger than that of the lava flows (ca. 0.24 ± 0.05 Ma) of the Cofre de Perote summit area, which supposedly represent the end of its activity. It must be assumed that the upper parts of the volcanic edifice collapsed in the Holocene, apparently unrelated to any volcanic activity of the central edifice. Therefore other triggers such as

earthquake shaking or unusual heavy rainfall must be considered as the initiating cause.

7.2. Los Pescados avalanche-lahar

This deposit consists of at least two different units that crop out along Los Pescados river valley forming a central terrace slightly dipping to the east. The deposit forms the lowermost channel-filling terrace deposit of Los Pescados River, and is therefore the youngest deposit in the area (Fig. 12B and cf. Hubbard et al., in press). It overlies a basaltic lava plateau, which has been

dated at 0.26 ± 0.03 Ma by the ^{40}Ar/^{39}Ar method, performed at the New Mexico Geochronological Lab. This lava is in contact with some irregular hills that form the northern river-valley wall that consists of basement limestone rocks (Fig. 12B). The southern wall comprises a prominent steep scarp composed of the older Las Cumbres avalanche, which at this location unconformably overlies a morphologically irregular and highly eroded rhyolitic ignimbrite.

The deposit consists of massive, heterolithologic mixture of boulders and coarse gravels within a silty–clayey matrix. Some blocks show jigsaw-fractures
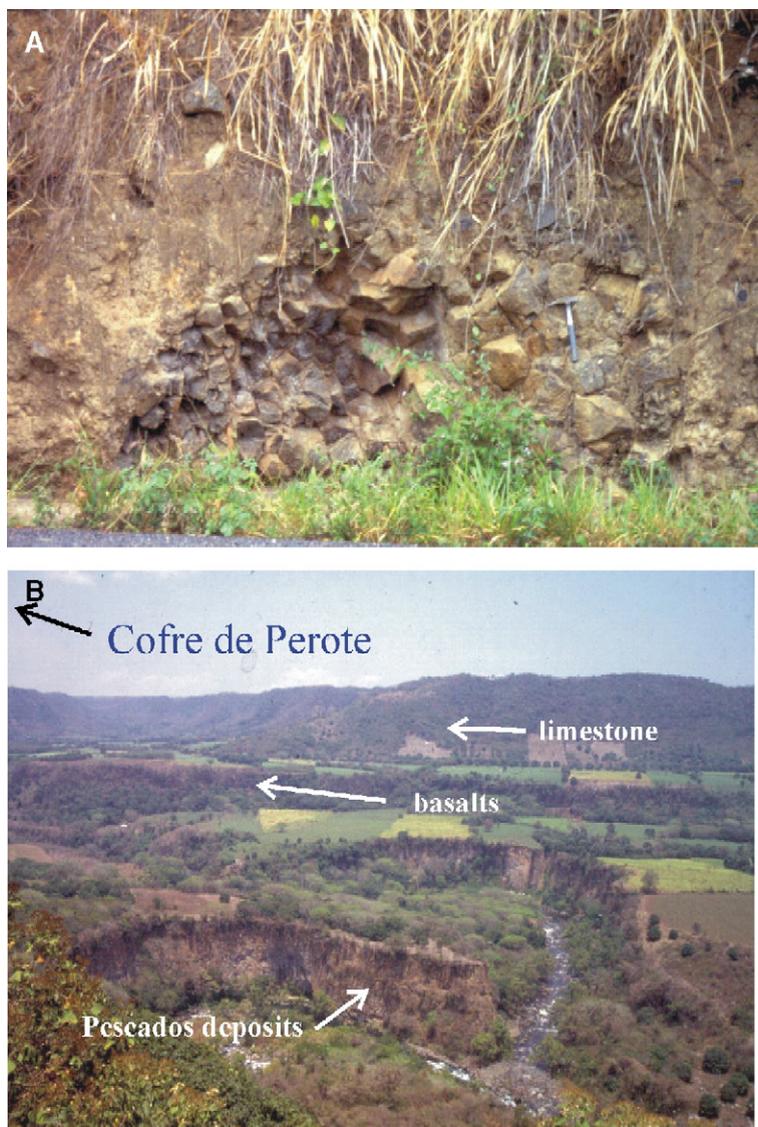

Fig. 12. Photographs of Los Pescados deposit. (A) Outcrop along Los Pescados River, about 30 km from source, showing a 1.4 m long block with jigsaw fracturing. (B) Panoramic view of Los Pescados northern river wall at the confluence with the Huitzilapan drainage, showing the Cretaceous limestone wall. The river-valley filled by an upper terrace composed of a horizontal basaltic lava flow that was incised and later filled by the Los Pescados deposit.

typical of debris avalanches (Fig. 12A); but there are no hummocks at the surface of this deposit. We consider that this deposit originated from a catastrophic edifice collapse and rapidly transformed to a lahar that flowed to a distance of at least 50 km from the Cofre de Perote source. Preliminary radiocarbon dates of charcoal samples collected within the deposit suggests an age of about 44,000 yr B.P. Considering that the last dated activity of Cofre de Perote occurred at ca. 0.24 Ma, this collapse took place long after the cessation of magmatic activity.

8. Instability of the Citlaltépetl–Cofre range

There are several factors that control edifice instability; some are related to magmatic activity like direct magma intrusion (Swanson et al., 1976; Elworth and Voight, 1996) or phreatomagmatic activity (Moriya, 1980), and others are associated with external processes such as steepening of slopes (Begét and Kienle, 1992), overloading from lava accumulation (Murray, 1988), hydrothermal alteration (Lopez and Williams, 1993; Day, 1996; Reid et al., 2001), gravitational spreading (Borgia, 1994; Van Wyk de Vries and Francis, 1997), and tectonic setting (Francis and Self, 1987; Carracedo, 1994; Tibaldi, 1995).

Instability can occur rapidly (months or up to a few years) associated with a discrete geologic event such as magmatic intrusion or a large seismic shock as in the case of Mount St. Helens in 1980 (Christiansen and Peterson, 1981) or the eruption of Bezymianny volcano (Belousov, 1996). However, instability can also develop over long periods of time due to the cumulative effect of several individual destabilizing factors, creating progressively unstable conditions that can be accelerated by the action of a sudden discrete event, such an earthquake.
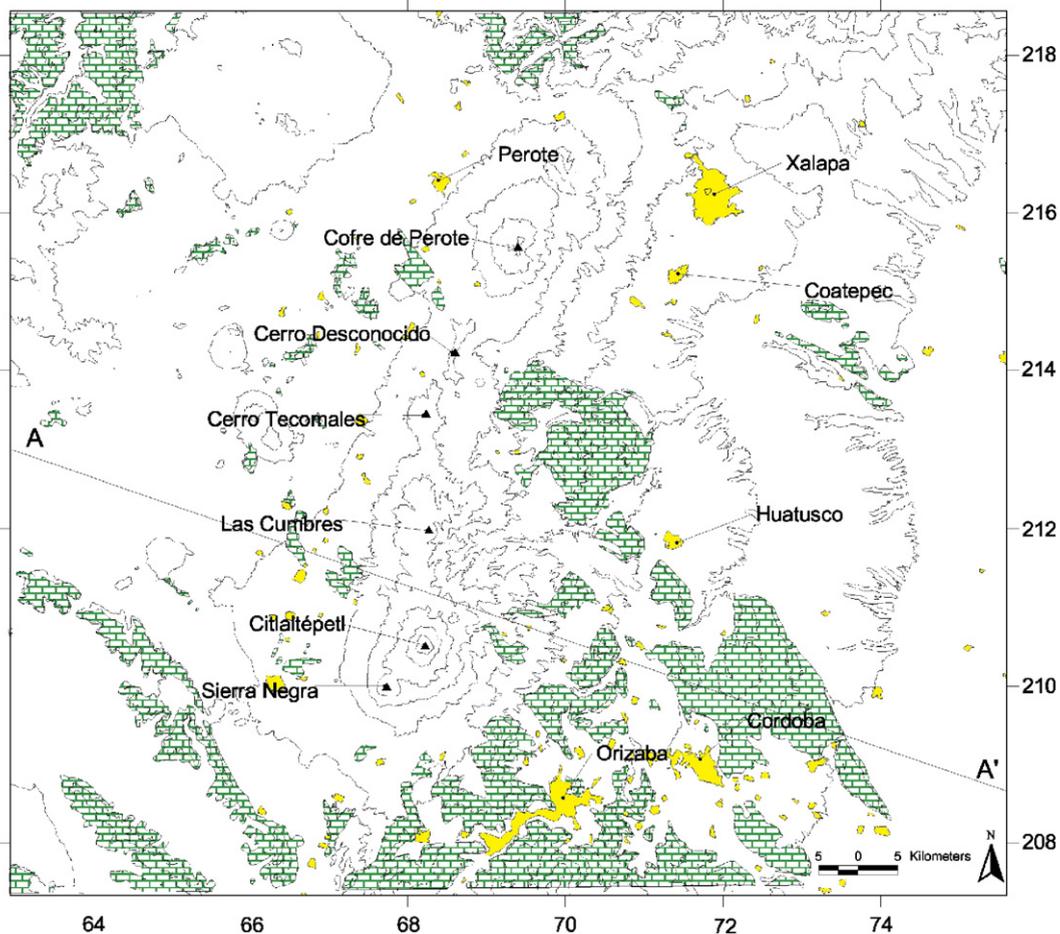

Fig. 13. Distribution of the limestone basement rocks (modified from Díaz-Castellón, 2003). In the Serdán-Oriental basin they are partially buried by pyroclastic and lacustrine deposits and have a higher altitude in comparison with equivalent rocks outcropping on the coastal plain. Section a–a' is shown in Fig. 14.

Several geologic factors contribute to an incremental slow development of instability in the CCPVR, the most important of which are: (1) the sloping basement rocks; (2) the regional tectonic stress field and structural setting; and (3) active hydrothermal systems and ancient epithermal alteration zones. Understanding the factors that provoke collapse is useful for hazard assessments that have the objective of mitigating loss of life and property.

8.1. Sloping basement

Volcanoes in the Cofre de Perote–Citlaltépetl range lie at the edge of the Altiplano. The contrasting physiographic relief between the Altiplano and the GCP, with more than 1200 m elevation difference, creates an initial preferential eastward anisotropy for gravity-driven flows in the area surrounding the CCPVR. Outcrops of the regional sedimentary basement rocks of Cretaceous age show low relief exposures at the Serdán-Oriental basin, which is in contrast with their higher relief exposures along the GCP (Fig. 13). In the coastal plain outcrops the relief becomes progressively lower towards the shore (Fig. 14A).

Geophysical data beneath the CCPVR provide additional information about the general structural configuration of the subsurface under the GCP (Mossman and Viniegra, 1976). They reveal a complex surface marked by a sloping substrate of Mesozoic age inclined towards the coast (Fig. 14B). This structural control produces a significant difference in relief and an asymmetric topographic profile that is inclined towards the east. Therefore, the exclusively eastward motion direction of major failure blocks is strongly influenced by the slope of the underlying basement, which shows a "down-dropped" displacement toward the coastal plain.

Preferential failure directions observed in the West Indies (Boudon et al., 2002) and Guatemala (Vallance et al., 1995) have similarly been attributed to the location of volcanoes above a regionally sloping basement. In the West Indies, this feature is due to the steeper slope of the islands toward the deep back arc Grenada Basin (Boudon et al., 2002). In Guatemala, this effect has been attributed to the position of volcanoes over inclined basements at the trenchward margin of the arc (Vallance et al., 1995). Modeling by Wooller et al. (2004) supports the field evidence of topographic effects by showing that edifice deformation processes can be influenced by minor basement slopes of as low as 1°.

8.2. Tectonic setting

In contrast with the western and central sectors of the MVB (Suter et al., 1991; Ferrari and Rosas-Elguera, 2000; García-Palomo et al., 2000), the eastern sector does not show evident structural patterns and no active
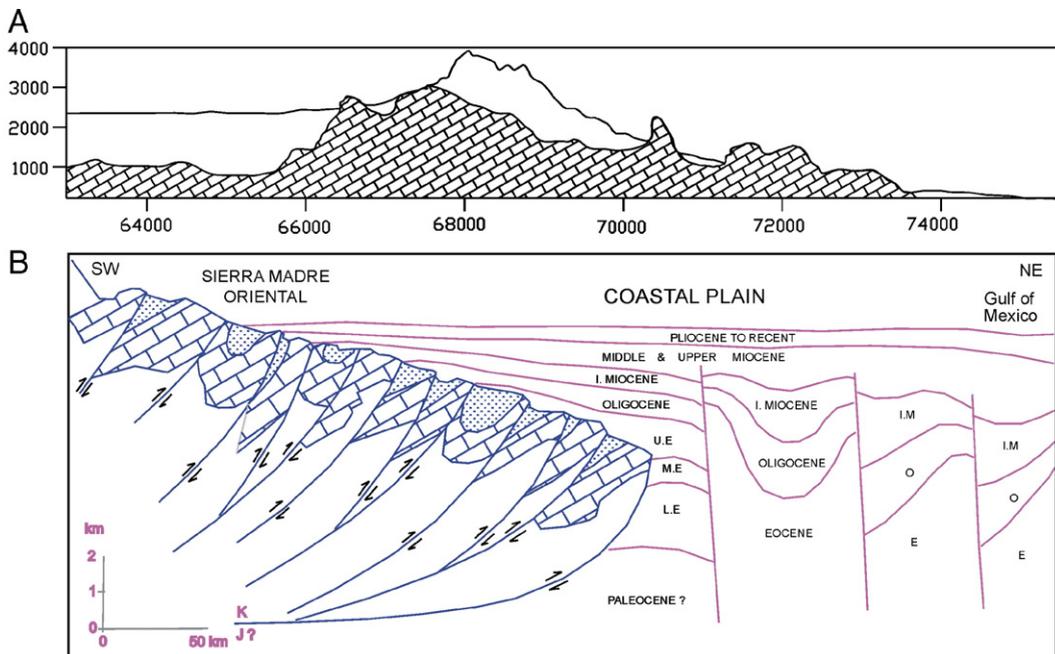

Fig. 14. (A) Schematic profile (traced on Fig. 13) showing the contrasting relief of the Altiplano, the coastal plain, and the outcrops of limestone basement sloping eastward. (B) Structural section of the Veracruz coastal plain (modified from Mossman and Viniegra, 1976).

faulting has been reported. However, some fracturing patterns and lineaments can be distinguished from satellite imagery interpretation (Negendank et al., 1985; Concha-Dimas et al., 2005) as shown in Fig. 15. A dominant NW direction corresponds with the structural domain that affects mostly Mesozoic sedimentary rocks. The two other important patterns oriented either E–W or ENE, both affect Quaternary volcanism. The CCPVR has been regarded as a N–S alignment of volcanoes. However, a careful inspection of the principal vent distribution (Fig. 1) clearly shows that the large volcanoes in fact follow two main

orientations: N–S (C. Desconocido–Las Cumbres–Citlaltépetl) and the NE (Citlaltépetl–Sierra Negra and Las Lajas–Cofre de Perote–C. Desconocido).

Based on the orientation of cone alignments following Nakamura (1977), we infer that the regional maximum horizontal stress direction is E–W in the southern portion of the eastern MVB, following the same trend of cone alignments and active faulting directions as in the central MVB reported by Suter et al. (1992). However, in the central and northern parts of the eastern MVB these trends are rotated to the ENE direction (Siebert and Carrasco-Núñez, 2002). These
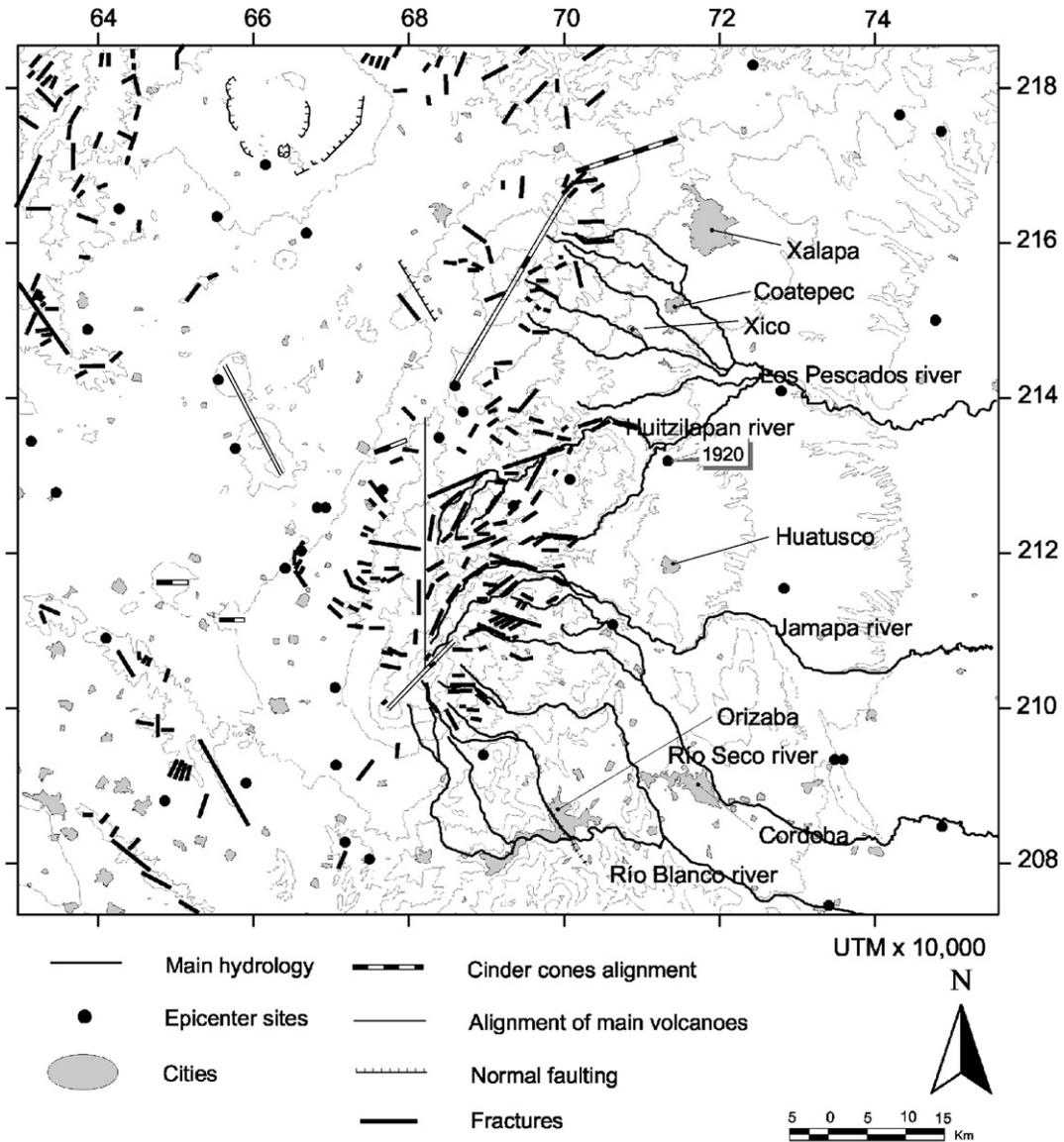

Fig. 15. Structural map showing the main fracture systems, volcano vent alignments, and distribution of earthquake epicenters (modified from Díaz-Castellón, 2003).
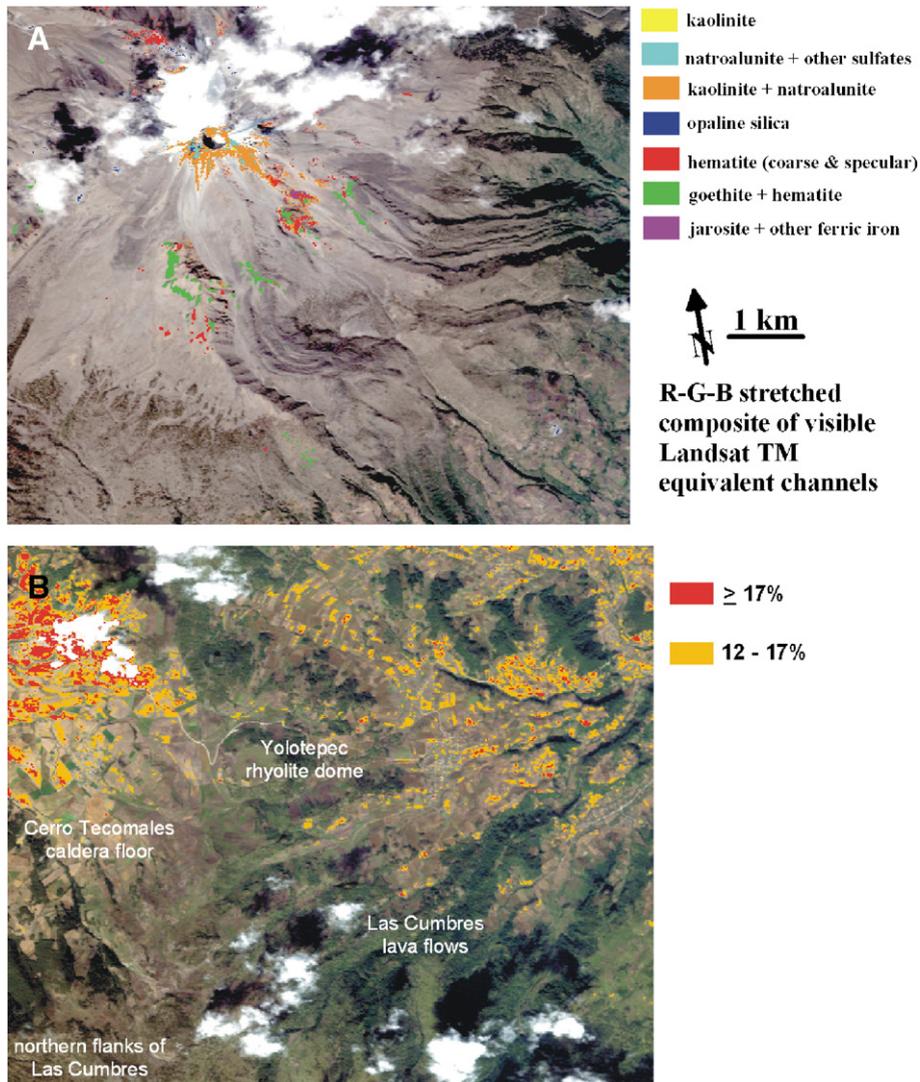
Fig. 16. (A) Alteration mineral map for Citlaltépetl (Pico de Orizaba) volcano using AVIRIS imagery (see text for details). (B) Remote sensing based estimates of halloysite in soil and weathered volcanic rocks of La Gloria area (see text for further details).

orientations must reflect the regional tectonic stress field. Likewise, Moriya (1980) found that the flank failure of over 30 Japanese volcanoes is perpendicular to the regional maximum horizontal compressive stress direction.

Although all the edifice collapses occurred towards the eastern sector of the CCPVR, the specific orientation of failure in each case varies and probably depends more on local structural conditions than on the regional tectonic setting. Likewise, magma uses fracture planes as pathways in complex ways relative to the regional stress field (Delaney et al., 1986), so that in some cases the alignment of cones, dikes, and flank vents do not always correspond to the regional maximum horizontal

stress. Thus, the models of Nakamura (1977) and Moriya (1980) can not be straightforwardly applied. For example in the case of Citlaltépetl volcano, mass movements related to the two major edifice failures were directed towards the NE drainage, an orientation that apparently does not show a direct relationship with the E–W trending regional stress inferred in this work. However, it is very possible that the final control on collapse direction is affected by the buttressing effect imparted by the older Sierra Negra volcano, located 7 km SW of Citlaltépetl volcano (Fig. 1), favoring collapse to the NE. In contrast, the Metlac failure was directed to the ESE flank of Citlaltépetl volcano, which is perpendicular to the alignment among Sierra Negra–

Citlaltépetl and the northeast outer domes (as shown in Fig. 3).

Las Cumbres avalanche was emplaced towards the east, perpendicular to the N–S trending alignment of the major volcanoes. This is in agreement with the orientation of faults underlying the main volcanic edifices, a direction which has been proposed to be perpendicular to the trend of cone breaching (Francis and Wells, 1988). Although in some cases, cone breaching may be parallel to the fault strike (Tibaldi, 1995; Lagmay et al., 2000). The N–S orientation of the CCPVR is nearly parallel to the NNW trending large normal Oaxaca fault (Nieto-Samaniego et al., 1995), however, a direct relationship between these two structural trends has not yet been documented.

In the case of Cofre de Perote, both the Xico and Los Pescados deposits resulted from flank failures directed to the SE, which is nearly perpendicular to the C. Desconocido–Cofre de Perote–Las Lajas alignment (Fig. 1). On the other hand, the ENE structural pattern, which is also nearly perpendicular to the ancient structural trend affecting mainly the basement rocks, is possibly an active system as it corresponds to the orientation of the prominent Huitzilapan fracture (Fig. 15). This feature is related to the 1920 earthquake and is parallel to the alignment of cinder cones located NE of Cofre de Perote. The SW end of this alignment is occupied by El Volcancillo cone that erupted in very recent times about 900 years ago (Siebert and Carrasco-Núñez, 2002). Epicenters of other historical earthquakes (Zúñiga et al., 1997) are aligned nearly parallel to this trend and are situated close to the Huitzilapan fracture, which reinforces the hypothesis that it is an active fault.

8.3. Hydrothermal alteration and chemical weathering

Despite the numerous processes that drive the destabilization of a volcanic edifice, some of the largest volume ($> 10^9$ m^3) collapses have occurred in volcanoes like Citlaltépetl, Mount Rainier and Mount Shasta (Cascade Range, USA) where extensive volumes of clay-rich hydrothermally altered rock were involved (e.g., Crandell, 1971; Lopez and Williams, 1993; Carrasco-Núñez et al., 1993; Scott et al., 1995; Crowley and Zimbelman, 1997; Crowley et al., 2003). Hydrothermal alteration can significantly weaken volcanic rocks by lowering their shear strength (Watters and Delahaut, 1995) and can replace primary phases with large volumes of hydrous minerals generated from prolonged contact with hot acidic fluids (Frank, 1983; Lopez and Williams, 1993; Zimbelman, 1996). These

minerals also provide cohesive strength for water-saturated debris flows, allowing them to travel tens of kilometers along river valleys without transforming to more dilute flows (Scott et al., 1995). A recent example of the effects of hydrothermal alteration is exemplified by the 1998 sector collapse of Casita Volcano, Nicaragua, where pervasive hydrothermal alteration over time decreased the stability of the summit zone, which rapidly collapsed in response to the unusually heavy and prolonged rainfall during the passage of hurricane Mitch (Sheridan et al., 1999; Van Wyk de Vries et al., 2000; Scott et al., 2005). Therefore, identification of the affected areas and the extent and intensity of alteration is important for pinpointing potential areas of instability.

Hydrothermally altered areas are well-exposed at the summit zones of Citlaltépetl (Fig. 16A) and Cofre de Perote volcanoes. At the active Citlaltépetl volcano hydrothermal processes are ongoing, producing an intense alteration of the summit area (Zimbelman et al., 2004). Also large exposures of altered rocks are associated with the remnants of prior edifices (Fig. 16A) (Hubbard, 2001). Although Cofre de Perote is a relatively old and extinct volcano, recent collapses have uncovered large parts of the summit's interior where prolonged hydrothermal activity has been focused. The 60 km^3 collapse of Las Cumbres has left a 4-km-wide ampitheater, now occupied by a dacite dome, with no evidence of hydrothermally altered areas detected by either remote sensing data or detailed field mapping (Rodríguez, 1998; Hubbard, 2001). Hubbard (2001) suggested that the original volume of hydrothermally altered rocks at Las Cumbres was largely removed during its collapse, and that the only remaining evidence of this process is in the matrix mineralogy of the debris avalanche and runout deposits.

Hubbard (2001) made the initial characterization of hydrothermally altered areas on Citlaltépetl volcano (Fig. 16A). Using Airborne Visible InfraRed Imaging Spectrometer (AVIRIS) hyperspectral data, a spectral library of minerals, and various spectral unmixing and shape-fitting processing methods, Hubbard (2001) mapped various mixtures of hydrothermal alteration minerals on the modern Citlaltépetl cone and the remants of the Torrecillas and Espon de Oro edifices. For example, kaolinite, alunite and hydrous silica minerals were mapped on the upper parts of Citlaltépetl; hematite, goethite, jarosite, and kaolinite were mapped in parts of Torrecillas; and kaolinite, hematite and hydrous silica were mapped in parts of the remnants of Espolon de Oro (Fig. 16A).

Zimbelman et al. (2004) later presented a more complete edifice stability assessment by determining rock mass strengths for the whole edifice. These authors found that alteration at the summit area is more pervasive within the fracture systems and includes acid sulfate, and advanced argilic, argillic, and silicification ranks. The crater interior consists of highly fractured layers of volcanic breccia, scoria, and both blocky and massive dacitic lava flows (Fig. 2B), all of which host extensive zones of replacement alteration including massive, funnel-shaped zones and thinner selvage zones bordering fractures. Silicification and advanced-argillic alteration processes are still occurring adjacent to the active fumaroles on the crater's outer west rim (Zimbelman et al., 2004). Further, volume estimates of altered material in the cone by numerical modeling ranged between 0.04 and 0.5 km^3.

La Gloria Volcanic Complex consists of the remains of two eroded stratovolcanoes. The southernmost edifice, Cerro Tecomales, shows evidence of Holocene activity that is possibly related to the same ENE structural regime responsible for the monogenetic volcanism located further east and north of the Los Pescados River. Although additional remote sensing and field mapping could improve the interpretation, preliminary field-based geologic mapping (Rodríguez, 1998) and AVIRIS remote sensing mapping (Hubbard et al., 2002) suggest that the dominant material at the surface is intensely weathered ash and lava flows with well-developed soil horizons. Recent volcanic centers exhibit only localized areas of hydrothermal alteration. Unlike other intensely weathered areas of the CCPVR and coastal plain with denser vegetation covers, deforestation and cultivation reveals the extent of weathered and hydrothermally altered volcanic deposits (Fig. 16B) in the area just upstream of the Huitzilapan River and 1920 earthquake epicenter. These places can provide source materials for future cohesive debris flows.

As in the case of Citlaltépetl volcano, Cofre de Perote has a well-exposed summit amphitheater (Fig. 11A) that shows different areas of argillic alteration, although these zones are not as extensive as on Citlaltépetl. A preliminary characterization of the alteration mineralogy in the summit area using 196 band EO-1 Hyperion data and Advanced Spaceborne Thermal Emission and Reflection Radiometer (ASTER) data (Díaz-Castellón et al., 2004) indicates the presence of three distinct zones of alteration dominated by (1) halloysite mixed with hydrous silica, (2) a mixture of halloysite and ferric iron, and (3) strong ferric iron. The Xico avalanche and Los Pescados deposit show the same minerals as the Cofre summit area plus kaolinite, smectite and natroalunite (Díaz-Castellón et al., 2004).

9. Implications for hazard assessment

Although large edifice collapse events are infrequent hazards, in volcanic regions they represent a catastrophic scenario (Siebert, 1984) that needs to be assessed in order to reduce the potential impact on populated areas.

The history of multiple edifice collapse events along the CCPVR indicates that this process was common during the Late Pleistocene times, and that the mass movement originated from different source areas under diverse conditions. Large volumes of volcaniclastic sediments were shed exclusively towards the eastern coastal plain in response to the predominant basement slope, local effect of morphostructural setting, and the distribution and intensity of rainfall enhanced hydrothermal alteration, and chemical weathering processes.

The products of edifice failure in the CCPVR include debris avalanches, debris flows, hyperconcentrated flows and avalanches that transformed directly into lahars. Although all of these are catastrophic in nature, their runout distances and inundation areas are quite variable. Thus a careful identification of the deposit type is important for developing a more precise hazard assessment. Although cohesive or clay-rich lahars and debris avalanches both may have origins as sector collapses, cohesive lahars with low H/L values have longer runouts and may spread more widely than debris avalanches with similar volumes. However, debris avalanches are normally much more voluminous. A combination of unstable conditions and variable triggering mechanisms are responsible of the various types of deposits produced from volcanic edifice failure and landslides.

The Metlac and Jamapa deposits from Citlaltépetl, and the proximal Las Cumbres deposits initiated as debris avalanches associated with sector collapses. The latter two are by far the most voluminous units yet reported in the literature. They were distributed widely as primary grain flows that transformed downstream to debris flows, and finally to hyperconcentrated flows. Although we have not found any direct evidence that relates the collapse events that occurred along the CCPVR with contemporaneous volcanic activity, it is possible that the most voluminous avalanche deposits had a magmatic component or an eruptive trigger that contributed to the energy needed to produce their relatively high mobility.

In contrast, the Teteltzingo deposit is a clay-rich lahar (from Citlaltépetl volcano) that originated by the rapid transformation of an avalanche descending from the upper summit area of an ancestral cone (Espolón de Oro). Evidence for this conclusion is the extensive areas of intense hydrothermally altered rocks within the deposit. It is very likely that instability developed progressively over long periods of time, but the process could have been accelerated by a sudden event such an earthquake and/or extraordinary periods of heavy rainfall.

In fact, landslides triggered by earthquakes are relatively common (Keefer, 1984; Schuster and Crandell, 1984). In cases such as the 1994 earthquake that occurred near the Nevado de Huila volcano in Colombia (Scott et al., 2001), thousands of small areas saturated by prolonged rainfall were ready to be mobilized. Although the resulting seismogenic flow along the Paez River had a relatively low volume, it produced a catastrophe because it traveled more than 100 km as it caused as many as 1000 casualties. The casualties estimated during the 1920 Huitzilapa debris flow range
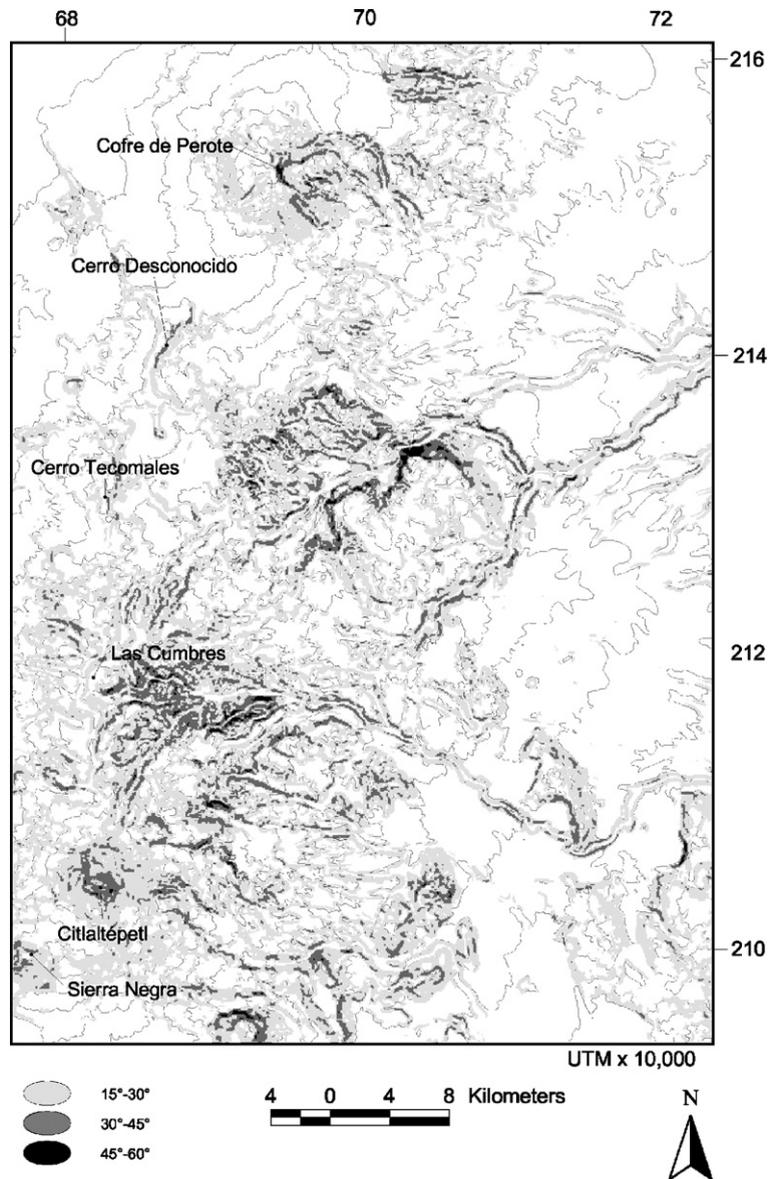

Fig. 17. Slope map of the eastern MVB indicating three different ranges of values: 15–30° for intermediate slope, 30–45° for high slope, and 45–60° for very high slopes that exceed all repose angles.

between 220 and 600 (Camacho and Flores, 1922). Although rainfall is unlikely to be a major factor during the generation of very large-volume collapses with deep-seated failure planes, it has been invoked as a triggering agent for many small-volume non-volcanic and volcanic landslides, such as the catastrophic 1998 collapse of Casita volcano in Nicaragua (Sheridan et al., 1999; van Wyk de Vries et al., 2000; Scott et al., 2005). A similar non-magmatic triggering mechanism may have been in play during the Cofre de Perote collapse events (Los Pecados and Xico) because they apparently occurred during the Quaternary (i.e.<43,000 yr B.P.), despite the long preceding period of inactivity of about 0.25 Ma.

Because Citlaltépetl is the only large active volcano of the CCPVR it should be considered as the most hazardous edifice in the region. This is particularly true due to its passive fumarolic activity, its present highly unstable summit cone with very steep slopes, and its large active glacier that can provide water saturation conditions. Its summit area is strongly fractured and shows extensive zones of hydrothermally altered rock masses (e.g., Carrasco-Núñez, 2000; Hubbard, 2001;

Zimbelman et al., 2004) that indicate large areas of weak rock with a high potential for failure (Zimbelman et al., 2004). Glaciated active volcanoes such as Citlaltépetl must be seriously considered as potential sources of highly mobile, hazardous clay-rich lahars, especially considering the extensive areas of hydrothermal alteration. Collapse can be triggered either by magmatic activity or by any of the other external factors already discussed. However, as we have described before, the entire volcanic range has unstable features that can easily be triggered by external factors, such as seismic activity or rainfall. These combinations of events are very likely to occur considering that the area is seismically active and the rainfall rates are occasionally extraordinarily high (Díaz-Castellón, 2003).

A slope map can rapidly identify and classify unstable areas (Fig. 17). Trajectories of potential debris flows can be delineating along the main drainage network by modeling different degrees of hazard. The model for this paper was generated by using the Flow-2D software (unpublished by Sheridan, 1986), which was adapted to work in a MS-Windows environment, using 1:250,000 scale cartography and Digital Elevation
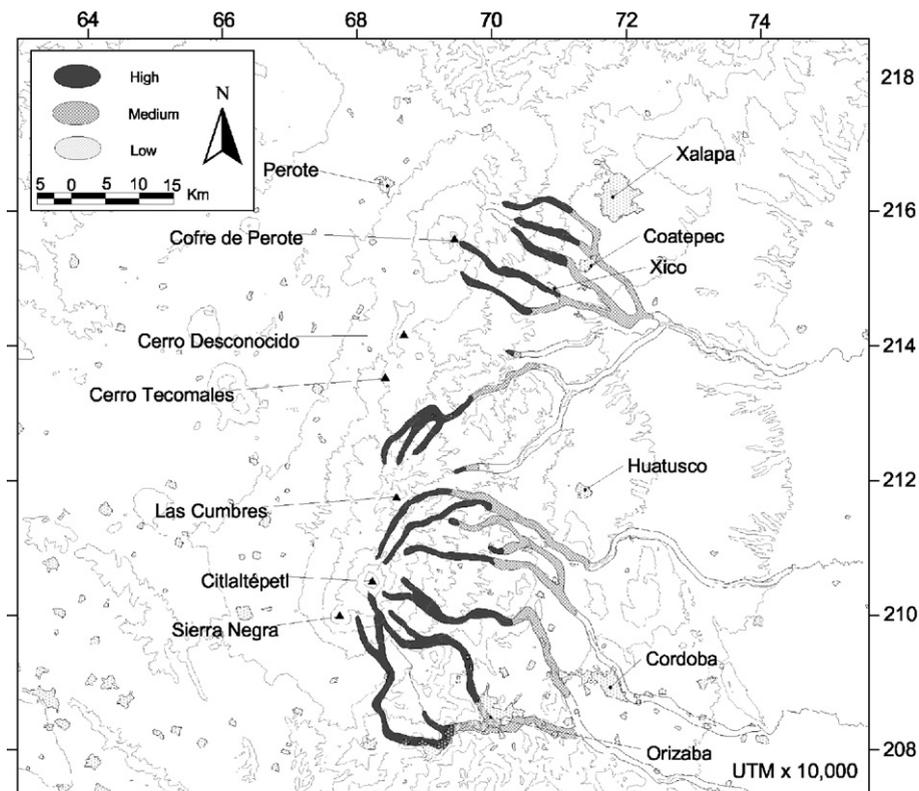

Fig. 18. Hazard map for debris flows of the CCPVR (modified from Díaz-Castellón, 2003) showing three different levels of hazard. High level is indicated in dark pattern, medium level is in grey pattern, and low level is in light colored pattern (see text for more details).

Models from INEGI with a resolution of about 90 m. We used several conditions to calibrate and generate three distinct scenarios for the hazard map (high, medium and low hazard) (Fig. 18).

Highly altered areas indicate zones where weak rocks are expected. It is important to note that the observed alteration is present mainly at summit areas, because widespread alteration on lower flanks or concealed in regions of gentle slope high on the edifice does not greatly facilitate collapse (Reid et al., 2001). A combination of alteration with slope gradient, fracture density, seismic data, and present morphology, allow us to identify some particularly instable areas along the CCPVR (Fig. 19).

Finally, it is important to emphasize that the failure of a volcanic edifice can occur without warning. This is particularly the case where there is clear evidence of unstable conditions such as irregular sloping basement, steep slopes and high gravitational gradients, strong stress regime, intense fracturing, extensively hydrother-

mally altered rocks, and water-saturated conditions. In these cases collapse can be triggered by nonmagmatic factors such as seismicity, unusual rainfall or by destabilization associated with the hydrothermal system.

10. Conclusions

Multiple collapse events have occurred along the Citlaltépetl–Cofre de Perote Volcanic Range during the late Pleistocene producing large volumes of volcaniclastic sediment that inundated the GCP. These catastrophic edifice collapses resulted from a combination of unstable conditions that developed over a long time period by the slow but progressive and cumulative effects of individual destabilizing processes. In contrast; they were apparently triggered by sudden discrete events such as earthquakes, heavy rainfall, or in a few cases by magmatic activity.

The collapse direction was solely towards the eastern coastal plain, principally in response to the highly
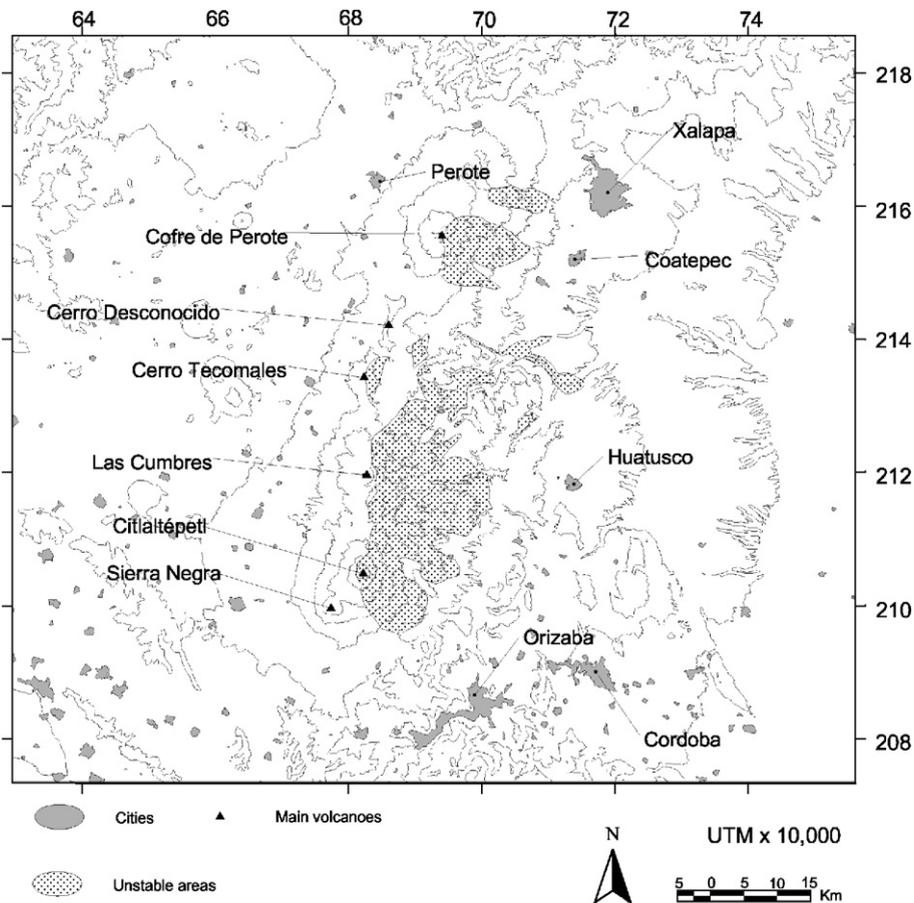

Fig. 19. Map showing the potential areas of instability based on the combination of unstable conditions including: slope, alteration areas, fractures, seismic data, and present morphology (modified from Díaz-Castellón, 2003).

irregular eastward slope of the basement rocks, and locally by the morphostructural setting. In addition to these factors, it is probable that reactivation of old structures affecting the pre-volcanic basement and the regional stress regime were also important controls for the eastward movement of the avalanches. Intense hydrothermal alteration, steep topography, and intense fracturing also may have played a role in the instability of the volcanic edifices forming the CCPVR in cases where non-magmatic triggers such as high precipitation rates and seismic activity were as important as volcanic activity.

Acknowledgements

References

Begét, J., Kienle, J., 1992. Cyclic formation of debris avalanches at Mount St. Augustine volcano. Nature 336, 701–704.

Belousov, A., 1996. Deposits from the 30 March 1956 directed blast at Bezimianny volcano, Kamchatka, Russia. Bull. Volcanol. 57, 649–662.

Borgia, A., 1994. The dynamic basis of volcanic spreading. J. Geophys. Res. 99, 17791–17804.

Boudon, G., Villemant, B., Komorowski, J.K., Ildefonse, P., Semet, M., 1998. The hydrothermal system at Soufiere Hills volcano, Monserrat (West Indies): characterization and role in the on-going eruption. Geophys. Res. Lett. 25, 3693–3696.

Boudon, G., Le Friant, A., Deplus, C., Komorowski, J.-C., Semet, M.P., 2002. Volcano flanks of the Lesser Antilles Arc collapse, some-times repeatedly: how and why: Montagne Pelee 1902–2002. Explosive Volcanism in Subduction Zones, St. Pierre, Martinique, May 12–16, 2002, p. 66. abstract volume.

Camacho, H., Flores, T., 1922. Memoria relativa al Terremoto Mexicano del 3 de Enero de 1920. Boletín del Instituto de Geológico de México, 38–39, 107 pp.

Cantagrel, J.M., Robin, C., 1979. K–Ar dating on eastern Mexican volcanic rocks; relations between the andesitic and the alkaline provinces. J. Volcanol. Geotherm. Res. 5, 99–114.

Capra, L., Macías, J.L., 2002. Failure of a natural dam: the 10 km cohesive debris flow originated from the Pleistocene debris avalanche deposit of Nevado de Colima volcano (Mexico): In Volcán de Colima, México, and its activity in 1997–2000. J. Volcanol. Geotherm. Res. 117, 213–235.

Capra, L., Macías, J.L., Scott, K.M., Abrams, M., Garduño, V.H., 2002. Debris avalanche and debris flow transformed from collapses in the Trans-Mexican Volcanic Belt, Mexico-behavior, and implications for hazard assessment. J. Volcanol. Geothem. Res. 113, 81–110.

Carracedo, J., 1994. The Canary islands: an example of structural control on the growth of large oceanic-island volcanoes. J. Volcanol. Geotherm. Res. 60, 225–241.

Carrasco-Núñez, G., 1993. Structure, eruptive history, and some major hazardous events of Citlaltépetl volcano (Pico de Orizaba), Mexico, (Ph.D. dissertation), Michigan Technological University, U.S.A., 182 pp.

Carrasco-Núñez, G., 2000. Structure and proximal stratigraphy of Citlaltépetl Volcano (Pico de Orizaba), Mexico. Special paper "Cenozoic Volcanism and Tectonics of Mexico" of the Geol. Soc. Amer. Bull. 334, 247–262.

Carrasco-Núñez, G., Gómez-Tuena, A., 1997. Volcanogenic sedi-mentation around Citlaltépetl volcano (Pico de Orizaba) and surroundings, Veracruz, Mexico. In: Aguirre-Díaz, G.J., Aranda-Gómez, J.J., Carrasco-Núñez, G., Ferrari, L. (Eds.), Magmatism and Tectonics in the Central and Northwestern México—a Selection of the 1997 IAVCEI General Assembly Excursions; México, D.F., UNAM, Instituto de Geol., Excursion, vol. 16, pp. 131–151.

Carrasco-Núñez, G., Vallance, J.W., Rose, W.I., 1993. A voluminous avalanche-induced lahar from Citlaltépetl volcano, México: implications for hazard assessment. J. Volcanol. Geotherm. Res. 59, 35–46.

Childs, F.S., 2005. Petrography and distribution of the Las Cumbres debris deposit, Veracruz, Mexico. M.A. report. University at Buffalo, NY.

Christiansen, R., Peterson, D., 1981. Chronology of the 1980 eruptive activity. U.S. Geol. Surv. Prof. Pap. 1250, 17–30.

Concha-Dimas, A., Cerca, M., Rodríguez, S.R., Watters, R.J., 2005. Geomorphological evidence of the incluence of pre-volcanic basement structure on emplacement and deformation of volcanic edifices at the Cofre de Perote-Pico de Orizaba chain and implications for avalanche generation. Geomorphology 72, 19–39.

Crandell, D.R., 1971. Postglacial lahars from Mount Rainier Volcano, Washington. U.S. Geol. Surv. Prof. Pap. 677. 75 pp.

Crowley, J.K., Zimbelman, D.R., 1997. Mapping hydrothermally altered rocks on Mount Rainier, Washington, with Airborne Visible/Infrared Imaging Spectrometer (AVIRIS) data. Geology 25, 559–562.

Crowley, J.K., Hubbard, B.E., Mars, J.C., 2003. Analysis of potential debris flow source areas on Mount Shasta, California, by using airborne and satellite remote sensing data. Remote Sens. Environ. 87, 345–358.

Day, S., 1996. Hydrothermal pore fluid pressure and the stability of porous, permeable volcanoes. In: McGuire, W.J., Jones, A.P., Neuberg, J. (Eds.), Volcano Instability on the Earth and other Planets: Spec. Publ.-Geol. Soc. Lond., vol. 110, pp. 77–94.

De la Cruz-Reyna, S., Carrasco-Núñez, G., 2002. Probabilistic analysis of Citlaltépetl eruptive activity. J. Volcanol. Geotherm. Res. 113, 279–290.

Delaney, P., Pollard, D., Ziony, J., McKee, E., 1986. Field relations between dikes and joints: emplacement processes and paleostress analysis. J. Geophys. Res. 91, 4920–4938.

Demant, A., 1978. Características del eje neovolcánico transmexicano y sus problemas de interpretación. Universidad Nacional Autónoma de México: Instituto de Geología Revista, vol. 2, pp. 172–187.

Díaz-Castellón, R., 2003. Análisis de la Estabilidad de Edificios Volcánicos del Flanco Oriental de la Sierra Citlaltépetl–Cofre de Perote. M.Sc. thesis Posgrado en Ciencias de la Tierra, Universidad Nacional Autónoma de México. 135 pp.

Díaz-Castellón, R., Hubbard, B., Carrasco-Núñez, G., Sheridan, M.F., 2004. Hydrothermal Alteration and Debris Flow/Avalanche Hazards at Cofre de Perote (México). IV. Reunión Nacional de Ciencias de la Tierra, Juriquilla, Querétaro (México). abstract volume, 145 pp.

Elworth, D., Voight, B., 1996. Evaluation of volcano flank instability triggered by dyke intrusion. Spec. Publ.-Geol. Soc. Lond. 110, 45–54.

Ferrari, L., Rosas-Elguera, J., 2000. Late Miocene to Quaternary extension at the northern boundary of the Jalisco block, western Mexico: the Tepic-Zacoalco rift revisited. In: Delgado-Granados, H., Aguirre, G., Stock, J.M. (Eds.), Cenozoic Tectonics and Volcanism of Mexico: Spec. Pap.-Geol. Soc. Am., vol. 334, pp. 41–64.

Ferrari, L., López-Martínez, M., Aguirre-Díaz, G., Carrasco-Núñez, G., 1999. Space-time patterns of Cenozoic arc volcanism in Central Mexico: from the Sierra Madre Occidental to the Mexican Volcanic Belt. Geology 27 (4), 303–306.

Francis, P.W., Self, S., 1987. Collapsing Volcanoes: Scientific American 256-6, 90–97.

Francis, P., Wells, A., 1988. LANDSAT Thematic Mapper observations of debris avalanche deposits in the Central Andes. Bull. Volcanol. 50, 258–278.

Frank, D., 1983. Origin, distribution, and rapid removal of hydrothermally formed clay at Mount Baker, Washington. U.S. Geol. Surv. Prof. Pap. 1022-E, 131 pp.

García-Palomo, A., Macías-Romo, J.L., Garduño, V., 2000. Miocene to recent structural evolution of the Nevado de Toluca volcano region, central Mexico. Tectonophysics 318 (1), 281–302.

Heine, K., 1988. Late Quaternary glacial chronology of the Mexican volcanoes. Die Geowissenschaften 7, 197–205.

Höskuldsson, A., Robin, C., Cantagrel, J.M., 1990. Repetitive debris avalanche events at Volcan Pico de Orizaba, México, and their implications for future hazard zones: IAVCEI, Mainz, Germany, International Volcanological Congress, abstract volume.

Höskuldsson, A., 1992. Le complexe volcanique Pico de Orizaba-Sierra Negra-Cerro Las Cumbres (Sud-Est Mexicain): Structure, dynamismes eruptifs et evaluations del areas. Ph.D. dissertation, University of Blaise Pascal, France. 210 pp.

Hubbard, B.E., 2001. Volcanic Hazard Mapping using Aircraft, Satellite, and Digital Topographic Data: Pico de Orizaba (Citlaltépetl), Mexico, Ph.D. dissertation, University at Buffalo, NY. 354 pp.

Hubbard, B.E., Sheridan, M.F., Scott, K., Crowley, J.K., Rodríguez, S. R., 2002. Cohesive debris flow hazards in the Huitzilapan-Pescados watershed, Eastern Trans-Mexican Volcanic Belt; Clay Minerals Society 39th annual meeting; abstracts, Program and Abstracts—Annual Clay Minerals Conference, Boulder CO, June 08–13.

Hubbard, B.E., Sheridan, M.F., Carrasco-Núñez, G., Díaz-Castellón, R., Rodríguez, S., in press. Comparatice lahar hazard mapping at Volcán Citlaltépetl, Mexico using SRTM, ASTER AND DTED-1 digital topographic data. J. Volcanol. Geotherm. Res.

Iverson, R.M., Schilling, S.P., Vallance, J.W., 1998. Objective delineation of lahar hazard zones. Geol. Soc. Amer. Bull. 110, 972–984.

Keefer, D.K., 1984. Landslides caused by earthquakes. Geol. Soc. Amer. Bull. 95, 406–421.

Komorowski, J.-C., Glicken, H.X., Sheridan, M.F., 1991. Secondary electron imagery of microcracks and hackly fracture surfaces in sand-sized clasts from the 1980 Mount St. Helens debris-avalanche deposit: implications for particle–particle interactions. Geology 19, 261–264.

Lagmay, A.M., van Wyk de Vries, B., Kerle, N., Pyle, D.M., 2000. Volcano instability induced by strike–slip faulting. Bull. Volcanol. 62, 331–346.

Lopez, D., Williams, S., 1993. Catastrophic volcano collapse: relation to hydrothermal alteration. Science 260, 1794–1796.

Lozano, L., Carrasco-Núñez, G., 2000. Evidencias de colapsamiento sectorial del Volcán Cofre de Perote. 7ª Reunión Internacional del Volcán de Colima, Abstract, p. 66.

Martínez, J.M., Avila, G., Agudelo, A., Schuster, R.L., Casadevall, T. J., Scott, K.M., 1995. Landslides and debris flows triggered by the 6 June 1994 Paez earthquake, southern Colombia. Landslide News 9, 13–15.

McGuire, W.J., 1996. Volcano instability: a review of contemporary themes. In: McGuire, W.J., Jones, A.P., Neuberg, J. (Eds.), Volcano Instability on the Earth and Other Planets: Spec. Publ.-Geol. Soc. Lond., vol. 110, pp. 1–23.

Moore, J.G., Clague, D.A., Holcomb, R.T., Lipman, P.W., Normark, W.R., Torresan, M.E., 1989. Prodigious submarine landslides on the Hawaiian Ridge. J. Geophys. Res. 94, 17465–17484.

Mooser, F., 1972. The Mexican Volcanic Belt: Structure and tectonics. Geofís. Int. 12, 55–70.

Moriya, I., 1980. Bandaian eruption and landforms associated with it. Collection of Articles in Memory of Retirement of Prof. K. Nishimura, Tohoku University, Tokyo, pp. 214–219.

Mossman, R.W., Viniegra, F., 1976. Complex fault structures in Veracruz province of Mexico. Amer. Assoc. Petrol. Geol. Bull. 60-3, 379–388.

Murray, J.B., 1988. The influence of loading by lavas on the sitting of volcanic eruption vents on Mt. Etna. J. Volcanol. Geotherm. Res. 35, 121–139.

Nakamura, K., 1977. Volcanoes as possible indicators of tectonic stress. J. Volcanol. Geotherm. Res. 2, 1–16.

Negendank, J.F.W., Emmermann, R., Krawczyk, R., Mooser, F., Tobschall, H., Werle, D., 1985. Geological and geochemical investigations on the Eastern Trans-Mexican Volcanic Belt. Geofis. Int. 24-4, 477–575.

Nieto-Samaniego, A.F., Alaniz, S.A, Ortega, F., 1995. Estructura interna de la falla de Oaxaca (México) e influencia delas anisotropías durante su actividad cenozoica. Rev. Mex. Cienc. Geol. 12, 1–8.

Oddone, E., 1921. La catastrofe sismica al Messico addi 3 gennaio 1920. Zeitschrift für Vilkanologie, band VI, Heft 2, 88–96.

Reiche, P., 1937. The Toreva block, a distinctive landslide type. Geology 45, 538–548.

Reid, M., Sisson, T., Brien, D., 2001. Volcano collapse promoted by hydrothermal alteration and edifice shape Mount Rainier, Washington. Geology 29, 779–782.

Rodríguez, S.R., 1998. El Campo Volcánico de Las Cumbres, al Oriente de la Faja Volcanica Trans-Mexicana: Evolución Geológica y Vulcanología de sus Principales Depósitos Piroclásticos. Ph. D. thesis, Posgrado en Ciencias de la Tierra, Universidad Nacional Autónoma de México. 263 pp.

Rodríguez-Elizarrarás, S.R., 2005. Geology of the Las Cumbres Volcanic Complex, Puebla and Veracruz states, Mexico. Rev. Mex. Cienc. Geol. 22, 181–198.

Schuster, R.L., Crandell, D.R., 1984. Catastrophic debris avalanches from volcanoes. Proccedings IV Symposyum on Landslides, Toronto, vol. 1, pp. 567–572.

Scott, K.M., Vallance, J.W., Pringle, P.T., 1995. Sedimentology, behavior, and hazards of debris flows at Mount Rainier, WashingtonU.S. Geol. Surv. Prof. Pap. 1547, 56 pp.

Scott, K.M., Macías, J.L., Vallance, J.W., Naranjo, J.A., Todríguez, S., McGeehin, J.P., 2001. Catastrophic debris flows transformed from landslides in volcanic terrains: mobility, hazard assessment, and mitigation strategiesU.S. Geol. Surv. Prof. Pap. 1630, 67 pp.

Scott, K.M., Vallance, J.W., Kerle, N., Macías, J.L., Strauch, W., Devoli, G., 2005. Catastrophic precipitation-triggered lahar at Casita volcano, Nicaragua: occurrence, bulking and transformation. Earth Surf. Processes Landf. 30, 59–79.

Scuderi, F., Sheridan, M.F., Hubbard, B., Rodríguez Elizarrarás, S., 2001. Las Cumbres Avalanche and Debris Flow Deposit, Mexico. Geol. Soc. Am. Abst. Progr. 33, 7.

Sheridan, M.F., Bonnard, C., Carrero, C., Siebe, C., Strauch, W., Navarro, M., Calero, J.C., Trujillo, N.B., 1999. Report of the 30 October 1998 rock fall/avalanche and breakout flow of Casita Volcano, Nicaragua, triggered by Hurracane Mitch. Landslide News 12, 2–4.

Siebe, C., Abrams, M., Sheridan, M., 1993. Holocene block-and-ash flow fan at the W slope of ice-capped Pico de Orizaba Volcano, Mexico: implications for future hazards. J. Volcanol. Geotherm. Res. 59, 1–31.

Siebert, L., 1984. Large volcanic debris avalanches: characteristics of source areas, deposits, and associated eruptions. J. Volcanol. Geotherm. Res. 22, 163–197.

Siebert, L., 2002. Landslides resulting from structural failure of volcanoes. In: Evans, S.G., DeGraff, J.V. (Eds.), Catastrophic Landslides: Geol. Soc. Am. Rev. Engin. Geol., vol. 15, pp. 209–235.

Siebert, L., Carrasco-Núñez, G., 2002. Late-Pleistocene to precolumbian behind-the-arc mafic volcanism in the eastern Mexican Volcanic Belt; implications for future hazards. J. Volcanol. Geotherm. Res. 115, 179–205.

Singh, S.K., Rodríguez, M., Espíndola, J.M., 1984. A catalog of shallow earthquakes of Mexico from 1900 to 1984. Bull. Seismol. Soc. Am. 74, 267–279.

Suter, M., Aguirre, G., Siebe, C., Quintero, O., Komorowski, J.C., 1991. Volcanism and active faulting in the central part of the Trans-Mexican Volcanic Belt. Field trip guide. Geol. Soc. Am. 224–243.

Swanson, D., Duffield, W., Fiske, R., 1976. Displacement of the south flank of Kilauea volcano: the result of forceful intrusion of magma into the rift zones. U.S. Geol. Surv. Prof. Pap. 963, 93 pp.

Tibaldi, A., 1995. Morphology of pyroclatic cones and tectonics in the con`uration of a volcanic arc. Terra Nova 4, 567–577.

Ui, T., 1983. Volcanic dry avalanche deposits-identification and comparison with nonvolcanic debris stream deposits. In: Aramaki, S., Kushiro, I. (Eds.), Arc Volcanism: J. Volcanol. Geotherm. Res. vol. 18, pp. 135–150.

Vallance, J.W., Scott, K.M., 1997. The Osceola mudflow from Mount Rainier; sedimentology and hazard implications of a huge clay-rich debris flow. Geol. Soc. Amer. Bull. 109, 143–163.

Vallance, J.W., Siebert, L., Rose, W.I., Girón, J.R., Banks, N.G., 1995. Edifice collapse and related hazards in Guatemala. In: Ida, Y., Voight, B. (Eds.), Models of Magmatic Processes and Volcanic Eruptions: J. Volcanol. Geotherm. Res., vol. 66, pp. 337–355.

van Wyk de Vries, B., Francis, P., 1997. Catastrophic collapse at stratovolcanoes induced by gradual volcano spreading. Nature 387, 387–390.

van Wyk de Vries, B., Kerle, N., Petley, D., 2000. Sector collapse forming at Casita volcano, Nicaragua. Geology 28, 167–170.

Watters, R.J., Delahaut, W.D., 1995. Effect of argilitic alteration on rock mass stability. Geol. Soc. Am. Rev. Engin. Geol. 139–150.

Wooler, L., van Wyk de Vries, B., Murry, J.B., Rymer, H., Meyer, S., 2004. Volcano spreading controlled by dipping substrata. Geology 32, 573–576.

Yáñez, C., García, S., 1982. Exploración de la región geotérmica Los Humeros-Las Derrumbadas, estados de Puebla y Veracruz. Comisión Federal de Electricidad. 96 pp.

Zimbelman, D.R., 1996. Hydrothermal alteration and it's influence on volcanic hazards: Mount Rainier, Washington, a case history. PhD thesis. University of Colorado at Boulder. 384 pp.

Zimbelman, D.R., Watters, R., Firth, I., Breit, G., Carrasco-Núñez, G., 2004. Stratovolcano stability assessment methods and results from Citlaltépetl, Mexico. Bull. Volcanol. 66, 66–79.

Zúñiga, F.R., Suárez, G., Ordaz, M., García-Acosta, V., 1997. Seismic Hazard in Latin America and the Caribbean. Mexico, IDRC/IPGH Report, 82pp. (part of the Global Seismic Hazard Assessment Program, GSHAP, International Decade for Natural Disaster Reduction. ONU).